Title
THE PRODUCTION OF DEUTERONS IN HIGH ENERGY NUCLEON BOMBARDMENT OF NUCLEI, AND ITS BEARING ON NUCLEAR CHARGE DISTRIBUTION

Author
Hess, Wilmot N.

Publication Date
1954-07-27

UNIVERSITY OF
CALIFORNIA

Radiation Laboratory

BERKELEY, CALIFORNIA

DISCLAIMER

UNIVERSITY OF CALIFORNIA

Radiation Laboratory

Contract No. W-7405-eng-48

THE PRODUCTION OF DEUTERONS IN HIGH ENERGY NUCLEON BOMBARDMENT OF NUCLEI, AND ITS BEARING ON NUCLEAR CHARGE DISTRIBUTION

Wilmot N. Hess
(Thesis)

July 27, 1954

Berkeley, California

Contents

THE PRODUCTION OF DEUTERONS IN HIGH ENERGY NUCLEON BOMBARDMENT OF NUCLEI, AND ITS BEARING ON NUCLEAR CHARGE DISTRIBUTION

Wilmot N. Hess

Radiation Laboratory, Department of Physics
University of California, Berkeley, California

July 27, 1954

ABSTRACT

A study has been made of deuterons produced at wide angles to a beam of 300 Mev neutrons and a beam of 300 Mev protons. The cross section dependence on atomic number for these deuterons for light elements can be written as $\sigma = kA^{1.2}$. This fact and the energy spectra and angular distribution of the deuterons show that the process that forms these deuterons is the indirect pickup process described by Bransden. This is a two step process in which the incident nucleon, or its collision partner, is scattered and then picks up in the same nucleus. A yield of tritons has also been observed that has the same A dependence and is presumably made by the same process. The A dependence of the deuteron production cross section also shows that these deuterons are made on the nuclear surface. Because of this fact, a comparison of the deuteron yields using an incident neutron beam and an incident proton beam can give information about the relative number of neutrons and protons on the surface of the nucleus. An analysis of this sort leads to the conclusion that for heavy nuclei there is a nuclear skin rich in neutrons. For light nuclei the effect is not present. If one assumes that this skin is composed only of neutrons its thickness must be about 0.8×10^{-13} cm for lead.

THE PRODUCTION OF DEUTERONS IN HIGH ENERGY NUCLEON BOMBARDMENT OF NUCLEI, AND ITS BEARING ON NUCLEAR CHARGE DISTRIBUTION

Wilmot N. Hess

Radiation Laboratory, Department of Physics
University of California, Berkeley, California

July 27, 1954

I. INTRODUCTION

Among the various phenomena which reveal the constitution and organization of the nucleus are the identity and characteristics of the secondary particles which emerge under controlled bombarding conditions. As examples of some aspects of nuclear organization which may be investigated by a study of secondary particles, one might mention the evaporation model and nuclear "temperatures", nuclear level densities and level widths, the characteristic momentum distributions for nucleons in nuclei, and at higher energies such considerations as cascade collision processes, mean free paths for particles in nuclear matter, and certain aspects of meson production.

The deuteron as a secondary particle has been of considerable interest, since its small binding energy invites questions as to the processes by which it may emerge intact, particularly in high-energy events. The elucidation of these phenomena has led to the "pickup" concepts which have been prominent in recent nuclear reaction theory.

In 1952 Clark at this laboratory observed a yield of deuterons at 40° to a 340 Mev proton beam from a carbon target.[1] Because these deuterons were made at a large angle to a high energy beam, it was improbable that they were direct pickup deuterons.[2,3] Direct pickup deuterons are formed when a nucleon having an energy of the order of 100 Mev enters a nucleus and interacts with one of the nucleons in the nucleus in such a way that the pair of nucleons on leaving the nucleus can exist as a bound state of a deuteron. It is quite apparent that if the nucleon in the target nucleus has a momentum parallel to the incident nucleon the probability of forming a deuteron is larger than if the momentum is

antiparallel or at right angles to the incident nucleon. The reason is that in this case the relative velocity of the two nucleons is smaller and it is more probable for them to fulfill the relative momentum conditions compatible with a deuteron. This means that in forming direct pickup deuterons, nucleons having momenta parallel to the beam of incident particles are favored. The direct pickup deuterons formed therefore are quite strongly peaked in the direction of the incident beam, with a moderately well defined energy related to the energy of the incident nucleons. Also, it is known that above 100 Mev the probability of making direct pickup deuterons decreases quite rapidly, so that at 340 Mev one would not expect to observe many of them at any angle. This is again related to the fact that the incident nucleon tries to find a partner nucleon of comparable momentum in the nucleus, and the higher the momentum of the incident nucleon the less likely it is to find such a partner. At about the time Clark first observed these deuterons, Bransden[4] wrote a theoretical paper describing a method for producing deuterons similar to those observed. Quoting from Bransden's paper, "Deuterons may be formed as the result of a second order process in which a nucleon of relatively small momentum (produced by the collision of the incident neutron with a nucleon in the target nucleus) picks up a second nucleon in the target nucleus to form a deuteron".

This formation mechanism could account for the observed deuterons. It is known that the energy spectrum of protons scattered from carbon at 40° to a 340° Mev proton beam shows considerable yields of protons of all energies below the bombarding energy.[5] These are due to collisions of the beam particles with target nucleons having various momenta so that scattered particles of various energies can be made.[6] Also, collision of a beam particle with more than one target nucleon occurs quite frequently. These collisions help produce the lower-energy scattered protons. From this evidence we know that there will be protons of the right energy to pick up partner nucleons traveling at 40° to the incident beam inside the target nucleus. These scattered protons can pick up partners having suitable momenta to make deuterons of the pair. The pickup process here forms deuterons traveling roughly in the direction of the scattered protons or, in this case, at 40° to the incident beam.

In this way we can make a sizable yield of deuterons, using a high energy nucleon beam at larger angles to the beam than the direct pickup process would allow. Such deuterons would be similar to those Clark observed.

It was decided to study these deuterons to see if the indirect pick-up process was responsible for their production and in general to determine their characteristics. The dependence on atomic number of the differential cross section for producing deuterons was measured, and the angular distribution and energy spectra of these deuterons were determined. In each case the experimental data agreed qualitatively with the indirect pickup process theory of Bransden and agreed well with a modified version developed in the course of this experiment. This provides strong evidence that the indirect pickup process is responsible for forming the observed deuterons. The A dependence of the cross section for producing these deuterons is of special interest. It was found that the differential cross section for making deuterons at 40° to the beam from various light elements could be written

$$\sigma_d (40^{\circ}) = kA^{1.2}$$

The fact that the exponent here is 1.2 is important. The comparable exponent for direct pickup deuterons is 0.41. Even for the scattered protons the exponent is only 0.72, because the nucleus is only partially transparent to the incident beam and some of the nucleons are not effective in the scattering process. The fact that the exponent 1.2 for the observed deuterons is considerably larger than 0.72 shows that the process that makes the observed deuterons must be a two step event such as the indirect pickup process. If the formation mechanism is the indirect pickup process the cross section can be written as the product of a scattering cross section for the incident nucleon and a probability for the pickup to occur. The two steps in the formation process are independent, so the probability that they both happen is the product of the probabilities that each one happens.

$$\sigma_{\substack{\text{indirect} \\ \text{pick up}}} = \left[\sigma_{\substack{\text{nucleon-nucleon} \\ \text{scattering}}}\right] \left[\begin{array}{c}\text{probability} \\ \text{that pick up} \\ \text{take place}\end{array}\right]$$

Now let us substitute in the A dependence power laws for each term in the equation above.

$$kA^{1.2} = \left[c_1 A^{.72}\right] \left[c_2 A^{.41}\right] = c_1 c_2 A^{1.13}$$

The reasonable agreement of the exponents here is strong evidence that the indirect pickup process is the formation mechanism for the observed deuterons. Furthermore, it is interesting to note that the A dependence of the pickup part of the indirect pickup process implies that the pickup takes place not throughout the whole volume of the nucleus, but only on the surface of the nucleus (and actually only on part of the surface). If only the surface nucleons are important in the process then, as we go to heavier target nuclei, the pickup probability should increase as the number of surface nucleons increases, or as $A^{2/3}$. Since the exponent is somewhat less than this, only part of the surface contributes to the pickup process. It seems reasonable that deuterons should be made only at the surface as the mean free path of deuterons in nuclear matter is small compared to nuclear dimensions (except for very low A). The fact that the pickup takes place on the nucleon surface suggests that some information about the surface can be obtained in the following way.

First, let us consider the indirect pickup deuterons resulting from proton bombardment. Figure 1a shows this event. For simplicity let us consider equal numbers of neutrons and protons in the nucleus. Then if the beam proton collides with the target proton both scattered particles are protons; if the beam proton collides with a target neutron, one proton and one neutron are scattered. This simple argument would lead one to expect three times as many scattered protons as neutrons in the scattered nucleon beam. This ratio is in reality somewhat different from 3:1, probably due to the values of the n-p and p-p differential cross section at 40°. Since most of the scattered nucleons are protons, then the particles that are picked up at the nuclear surface to form deuterons are mostly neutrons.

Next, if we perform a similar experiment using an incident neutron beam, as shown in Fig. 1b, we find a somewhat different situation.

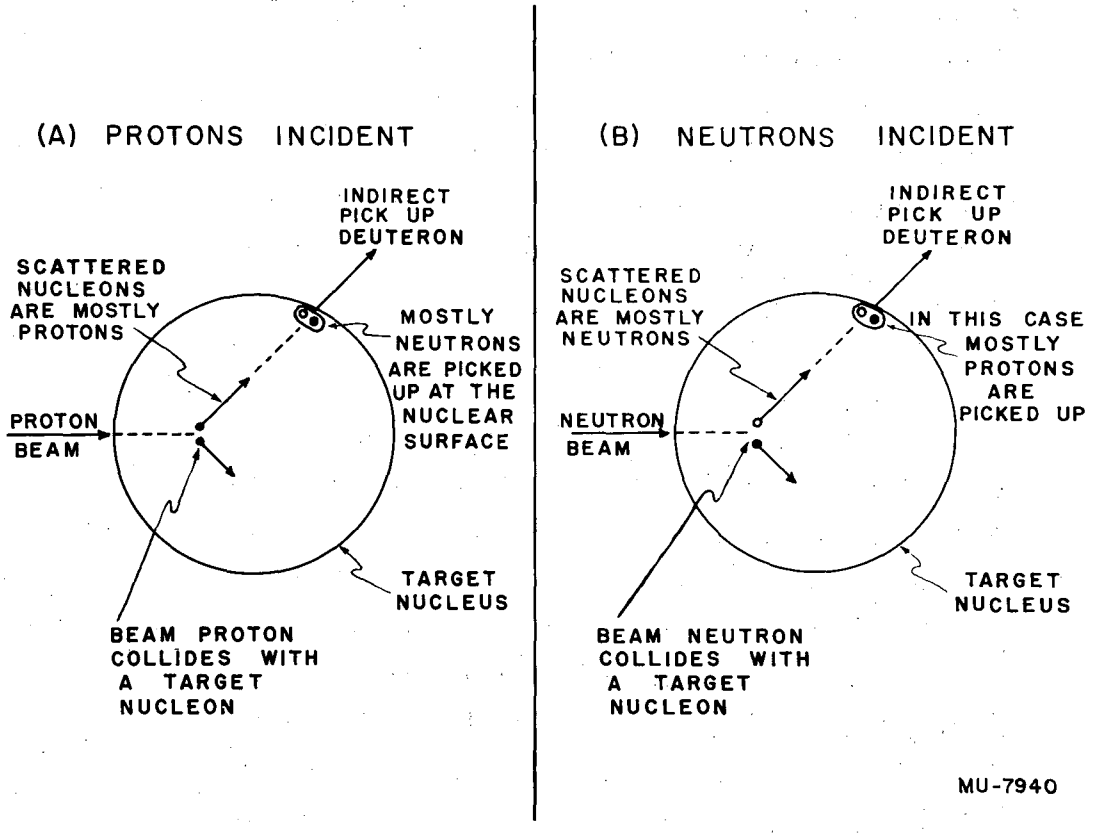

Fig. 1 Schematic Diagram of the Indirect Pickup Process Using (a) a Proton Beam or (b) a Neutron Beam Incident on the Target.

The same argument here would lead one to expect more scattered neutrons than protons in a ratio of 3:1. If the n-n differential cross section is the same as the p-p differential cross section (as charge symmetry arguments would lead one to believe), then this ratio would be exactly the reverse of the ratio for an incident proton beam. With a neutron beam incident the scattered nucleon beam consisting mainly of neutrons must pick up protons at the nuclear surface to form deuterons. In this way the yield of deuterons from a proton beam experiment depends upon the presence of neutrons on the nucleon surface, and the deuterons from a neutron beam experiment depend upon the presence of protons on the nuclear surface. If there are more neutrons than protons on the surface of the nucleus more deuterons will be made when a proton beam was used than when a neutron beam is used. Performing the neutron beam and proton beam experiments and using a somewhat more elaborate analysis led us to the conclusion that for heavy nuclei the fraction of surface nucleons that are neutrons is larger than the number of neutrons in the nucleus divided by the atomic number, indicating that there is a surplus of neutrons on the surface of the nucleus. There is no such effect for light nuclei.

There is a theoretical reason for believing that there may be a surplus of neutrons on the surfaces of heavy nuclei.[7] If one assumes that the nuclear part of the potential well of a nucleus is the same for neutrons and protons, and considers a well that is not square but has sloping sides (which is physically realistic), then the only difference between the total potential seen by neutrons and protons is the Coulomb potential. Adding the Coulomb potential to the nucleon well elevates the potential depression to which the protons are subject, and effectively pushes in the sides of the well for protons of a given binding energy, because of the sloping sides of the nucleon part of the potential. This means that protons are limited to a smaller space than neutrons of the same binding energy and, therefore, predicts a surface surplus of neutrons. This will be true only when the Coulomb potential is large, which is the case for heavy nuclei.

II. EXPERIMENTAL APPARATUS AND PROCEDURE

A. General Operating Conditions

1. Cyclotron Beams

This experiment was performed using the external high-energy proton and neutron beams of the 184 inch Berkeley synchrocyclotron. A plan view of the cyclotron showing the external proton beam is represented in Fig. 2 and in Fig. 3 a similar view shows the external neutron beam.

When a proton beam was used it was brought out into the external experimental area, called the "cave", by scattering.[8] The scattered proton beam has a longer pulse than an electrically deflected beam. This is desirable in the supression of accidental counts in any coincidence counting experiment. The energy of the proton beam was reduced from 340 Mev to 300 Mev by placing a copper energy degrader at the position shown in Fig. 2 and adjusting the bending magnet current appropriately. This was done to allow direct comparison with the neutron-beam experiments. The proton beam was monitored by using an argon-filled ionization chamber connected to a recording electrometer.

The neutron beam used in this experiment was produced by bombarding a 2 inch thick Be target with 340-Mev protons. The neutron spectrum* obtained this way is shown in Fig. 4. The peak of the spectrum is just about 300 Mev, which is the same energy as the proton beam used. The neutron beam was monitored in terms of the thermal neutron flux it produces in the shielding by using two BF_3-lined proportional counters placed as shown in Fig. 3 and counting the alpha particles from the reaction $B^{10}(n, \alpha) Li^7$. The BF_3 counter outputs were fed through amplifiers to scalers and recorded. The two counters tracked each other very well.

2. Targets

The targets used were lithium, carbon, aluminum, copper, cadmium, lead, uranium and polyethylene = $(CH_2)_n$. All the targets had less than 0.5 % contaminants. They were all 2-1/2 inch x 2-5/8 inch area

*This was obtained by Ball, Cladis and Hess by the method given in Cladis, Hadley, and Hess, Phys. Rev. 86, 110 (1952).

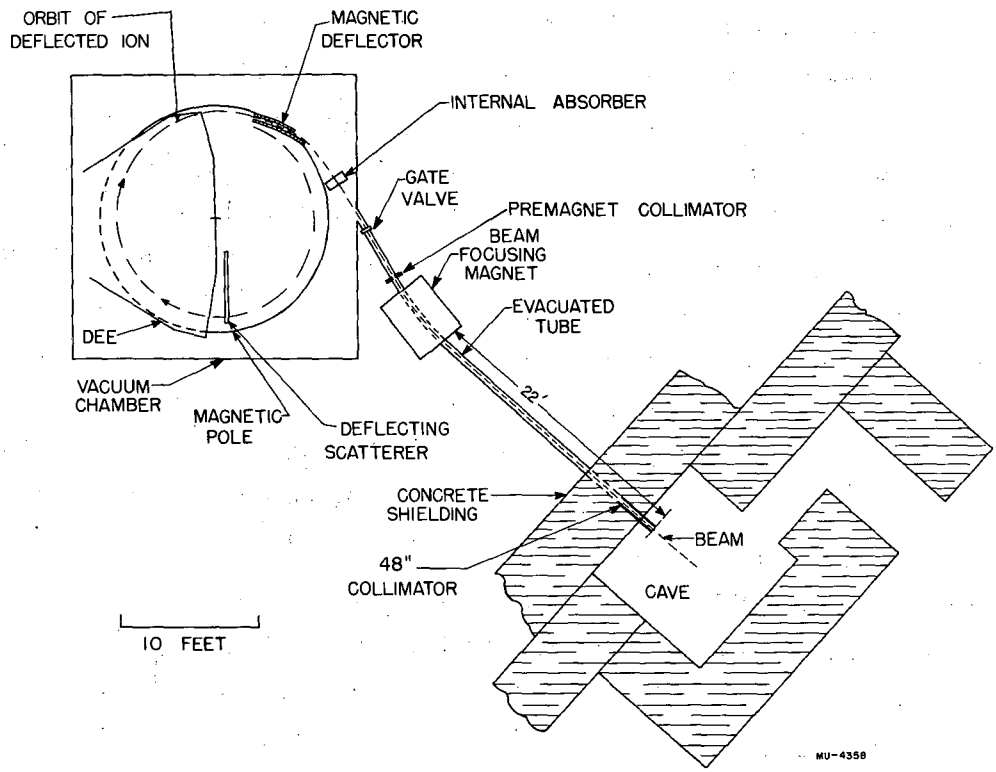

Fig. 2 Plan View of the Cyclotron Showing the External Proton Beam.

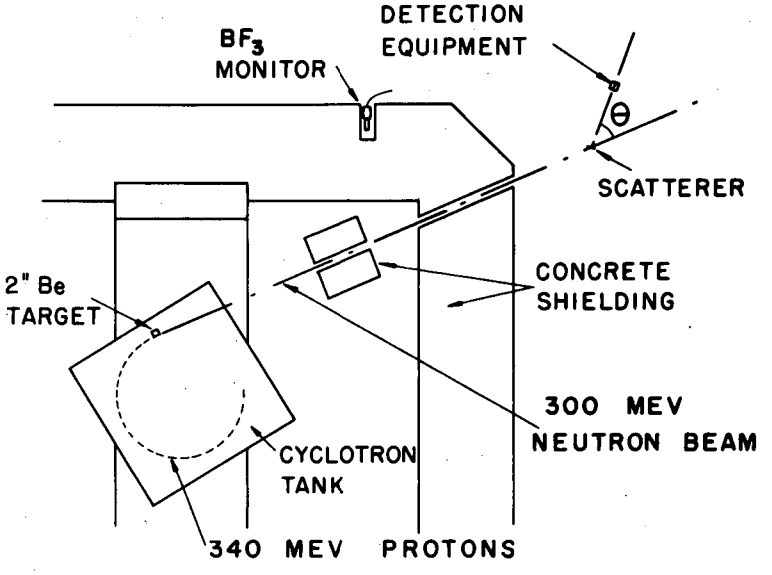

Fig. 3 General Experimental Arrangement for the Neutron Beam Experiment.

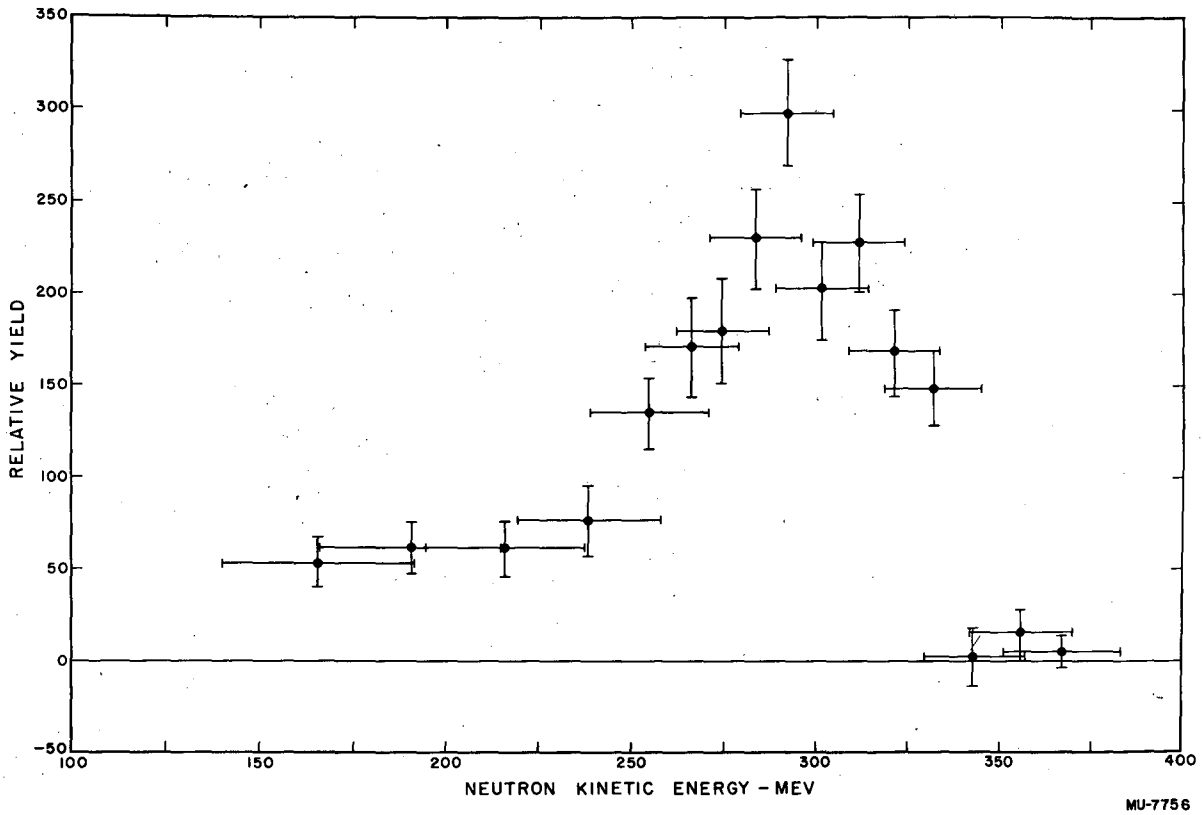

Fig. 4 Neutron Energy Spectrum Produced from 340 Mev Protons Bombarding 2" of Be.

which is larger than the beam areas used. They were all 9 Mev thick for 40 Mev deuterons except the lithium target, which was 7 Mev thick at the same energy. The lithium was machined and stored under mineral oil but picked up an estimated 2 % by weight of oxygen over the period of use. The surface of this target was cleaned before each run. Corrections were made accordingly, but proved negligible.

B. E - dE/dx Method for Particle Identification

1. General Experimental Method

A large part of the information in this experiment was obtained by a particle detection method which measured dE/dx and E for the scattered charged particles. This is accomplished by using a telescope of three crystal scintillators, the crystal towards the target moderately thin and the second crystal thick enough to stop most of the scattered particles. The third crystal is used to detect the passage of particles too energetic to be stopped in the second crystal. This third crystal was needed because the second crystal had to be kept to a reasonable size; to have stopped 300 Mev protons, the second crystal would have to have been 25 inches thick. The apparatus is shown in Fig. 5. The particle energy loss in the thin crystal is proportional to dE/dx and the energy loss in the second crystal is proportional to E of the incident particle. The measurement of these two parameters determines the mass and energy of the observed scattered particles. The relationship between E and dE/dx for various particles is plotted in Fig. 6. Actually the values plotted are the energy losses in the first two crystals. These are similar to, but not equal to, $\frac{dE}{dx}$ and E. It is seen from this figure that protons of energy greater than 35 Mev can be observed. Deuterons of energy 47 Mev up to 150 Mev fall on the hyperbola-like curve; above 150 Mev the deuterons may be confused with protons. Tritons of energy 58 Mev to 180 Mev can also be identified. The proton curve changes direction when the protons become energetic enough to pass through the E crystal.

2. Counters

The scintillators used in this experiment were made of terphenyl embedded in polystyrene plastic. This material is convenient to work with, is easily machined, is quite transparent, and produces pulses about

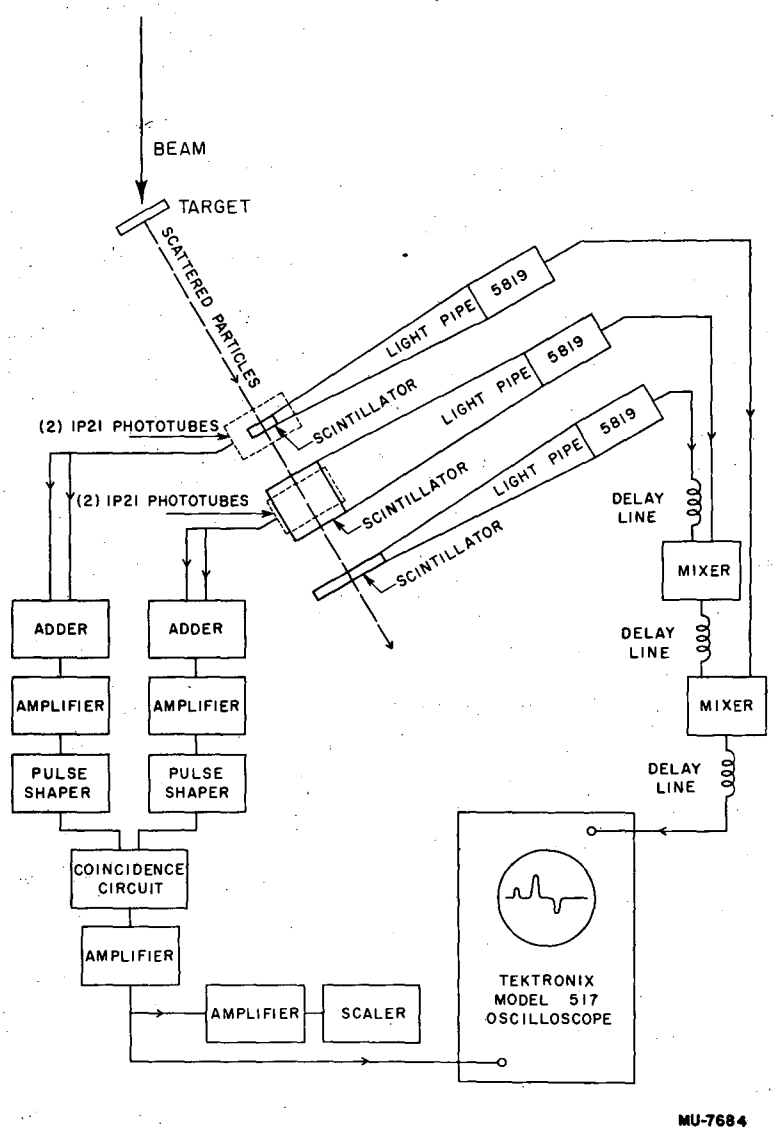

Fig. 5 Experimental Apparatus Used in the E-$\frac{dE}{dx}$ Method.

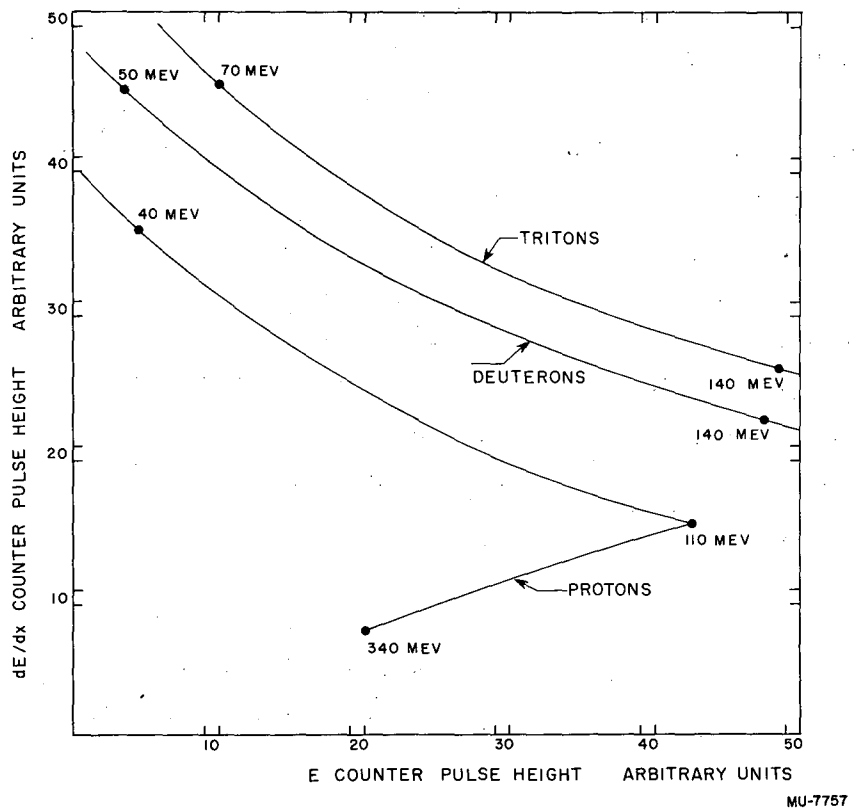

Fig. 6 The E- $\frac{dE}{dx}$ relationship for Various Particles.

2×10^{-8} second long. All three scintillators were viewed by RCA 5819 photomultipliers joined to the scintillators by tapered lucite light pipes. The first and second scintillators that measure dE/dx and E of the incident particles were also viewed by a pair of 1P21 photomultipliers on each scintillator. All the photomultipliers were magnetically shielded. The dE/dx scintillator which was closest to the target was made with the smallest area. It was 1.5 inches by 1.5 inches as seen by the scattered particles. The E scintillator had an area of three inches by three inches and the third or "pass through" counter had an area of four inches by four inches. In this way the effects of small angle scattering were minimized. Earlier attempts to use dE/dx counters about the same area as the E counter led to considerably greater variation in pulse height. The dE/dx scintillator was made thick enough so that the pulse height variation resulting from the Landau effect[9] and from photoelectron statistics in the phototube would not be serious enough to interfere with particle identification. At the same time, it was made no thicker than necessary so that the counter telescope could identify as low energy scattered particles as possible. A value of .4 in. for this counter was decided on after also trying .6 in. and .2 in. Because of the thickness of the $\frac{dE}{dx}$ crystal the particles that passed through the telescope had the following low energy cutoffs:

Protons: $E > 36$ Mev
Deuterons: $E > 48$ Mev
Tritons: $E > 58$ Mev

He^3 and heavier particles were not observed in any measurable quantity, probably because the energy cutoff gets so high. The energy cutoff for He^3 is 125 Mev. The E crystal was made 3 inches thick. This value was chosen because it was known that most of the deuterons to be studied in this experiment would be stopped by this thickness and that if the crystal were made much thicker the pulse height variation due to particles going through different parts of the crystal might become large.

3. Electronics

Figure 5 shows the electronics used with the $E - \frac{dE}{dx}$ equipment. The pulses from the 5819 photomultipliers viewing the scintillators were delayed about 10^{-7} second with respect to each other by using 100 foot lengths of cable then mixed in resistor networks and exhibited on a model 517 Tektronix oscilloscope. The 1P21 signals were used to trigger the scope. The distributed amplifiers in the 517 oscilloscope were used in presenting the 5819 phototube pulses. In this way the only means by which the pulse sizes from the 5819 tubes could vary were by a change in the voltage on the tube or by the scope amplifiers' changing characteristics during the experiment. The voltages were checked several times during the experiment, and varied less than five volts in about 1,000 if at all. The scope amplifiers were checked by using a pulse generator before and after the experiment to calibrate the scope deflection sensitivity. No change was observed in the sensitivity. A change of 2 % would have been seen.

The oscilloscope trigger circuit was arranged in such a way that when a fast particle went through the dE/dx and E scintillators the oscilloscope was triggered. The signals from these two 1P21 tubes attached to each scintillator were passed through a triode adder circuit (similar to the mixer circuit shown in Fig. 11*.) This circuit also limits the pulse size by cutting off the triode. The outputs of these circuits were amplified in Hewlett Packard Model 460 B distributed amplifiers and then fed through a second adder-limiter circuit. This circuit also clipped the pulse length to 10^{-8} second; a 58 in. length of 197 Ω coacial cable on the input grid provides this clipping action. This system of two adder-limiters and an amplifier was used to provide equal size pulses into a coincidence circuit, although the pulse sizes out of the 1P21 phototubes varied in height by as much as a factor of 100. The coincidence circuit was a germanium diode doubler circuit (shown in Fig. 11). The resolving time, which is limited by the input pulse length was about 2×10^{-8} second. In order that the coincidence circuit should have uniform efficiency for particles of different energy it was necessary to delay the dE/dx

*The fast electronics used in this experiment was similar to that designed and used at this laboratory by Drs. Bandtel, Frank, Godfrey and Madey.

1P21 signal by five feet of 197 Ω cable (about 0.5×10^{-8} second). In this way even a 5 Mev deuteron which took 0.8×10^{-8} second to go from the dE/dx crystal to the E crystal, produced a sizable pulse out of the coincidence circuit. The output from the coincidence circuit was fed through two Hewlett Packard Model 460 A distributed amplifiers and then into the scope trigger amplifier. The trigger amplifier on the scope was set so that single pulses from the coincidence circuit just would not trigger the sweep. The discriminator on the scaler which was counting the pulses from the coincidence circuit was set in the same way. The counts on this scaler tracked the number of scope traces to within 1 %. The output from the coincidence circuit was also recorded on a scaler.

4. Calibration

Part of one run was devoted to calibrating the E - dE/dx equipment. This was done by placing the scintillators directly in a low intensity beam of monoenergetic particles in the cave (see Fig. 2). Deuterons were accelerated to 190 Mev in the cyclotron and then the energy of the deuterons was reduced by placing copper energy degraders in the deflected beam. In this way deuterons of 120 Mev and 50 Mev were obtained in the cave. Similarly, the 340 Mev proton beam was reduced to 110 Mev and to 40 Mev. The pulse height distribution produced in the counters was measured for these various incident particles. The results of these measurements are shown in Fig. 7. The 40 Mev proton beam pulse height distribution is not shown because it was so poor. Range straggling, neutrons and other undesirable events obscured the pattern here. This is not surprising because the copper energy degrader in this case is 0.975 of a range thick. The center point of the 40 Mev proton distribution is shown. It is observed on Fig. 7 that the 120 Mev deuteron and 110 Mev proton distributions do not overlap. The tails on the distributions in Fig. 7 are probably due to scattering in the E crystal. The curves drawn on Fig. 7 are the E - dE/dx relationship plotted on Fig. 6. The theoretical curves have been fitted to the calibration data at the 110 Mev proton point. It is seen that the theoretical curve fits the experimental data quite well. Two corrections have been made to the theoretical E - dE/dx curves. First, saturation effects in the scintillator must be considered. A certain energy loss near the end of a particle's range does not produce as much light as the same energy loss would further from the end of the range.

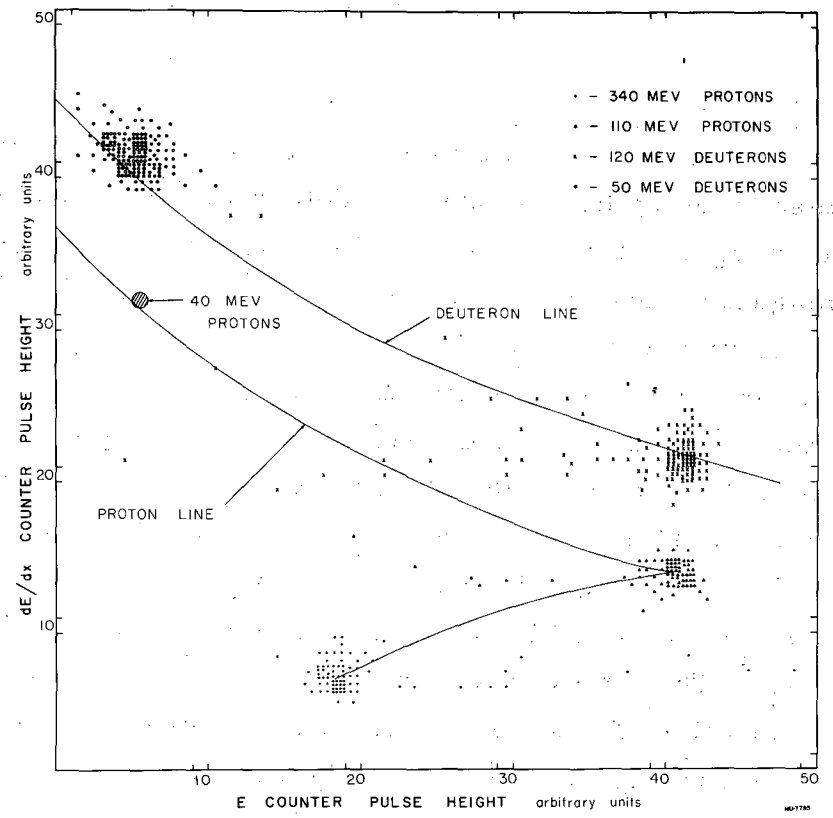

Fig. 7 E- $\frac{dE}{dx}$ Calibration Data Taken with Various Monoenergetic Beams.

The magnitude of this effect has been determined by Taylor and co-workers for anthracene.[10] The saturation effects in the present experiment have been corrected for by use of this same curve. Secondly, the scope gain is not linear for large deflections. This gain curve has been determined and corrected for. The voltages on the 1P21 photomultipliers were adjusted during the calibration run. The threshold for producing the trigger signal was determined for the five calibration points. The highest threshold was 1100 volts. The data were taken with the voltage at 1500 volts. This operating condition was well on a plateau. The 5819 voltages were set at values that gave convenient pulse sizes on the oscilloscope.

C. Hρ - Range Method

Part of the data taken using the 300 Mev proton beam were obtained by using Hρ and range to determine the scattered particle mass and energy. This was done by bending the scattered particles through a magnetic field and then counting the number of particles that appeared at various exit positions by a 35 channel set of scintillation counters. This equipment is quite similar to that used by Cladis.[5] The separation of deuterons from protons was accomplished by placing wedge-shaped absorbers in front of the 35 channel counters. Fig. 8 shows the experimental arrangement. The absorbers were made to be a certain fraction of a deuteron range thick at each point. Several of these wedge shaped absorbers were made having thicknesses of $0.3R_D$, $0.6R_D$, $1.2R_D$ and $2.0R_D$. The total counting rate of the 35 channel counters was determined as a function of absorber thickness. A curve of this sort for aluminum is shown in Fig. 9. The dip at the deuteron range is quite apparent indicating that there is a measurable fraction of deuterons.

The table below shows how the range varies for different particles that have the same Hρ.

Particle	$\frac{\text{Momentum of Particle}}{\text{Momentum of Deuteron}}$	$\frac{\text{Range of Particle}}{\text{Range of Deuteron}}$
Proton	1	5.90
Deuteron	1	1.00
Triton	1	0.35
He^3	2	1.05
He^4	2	0.50

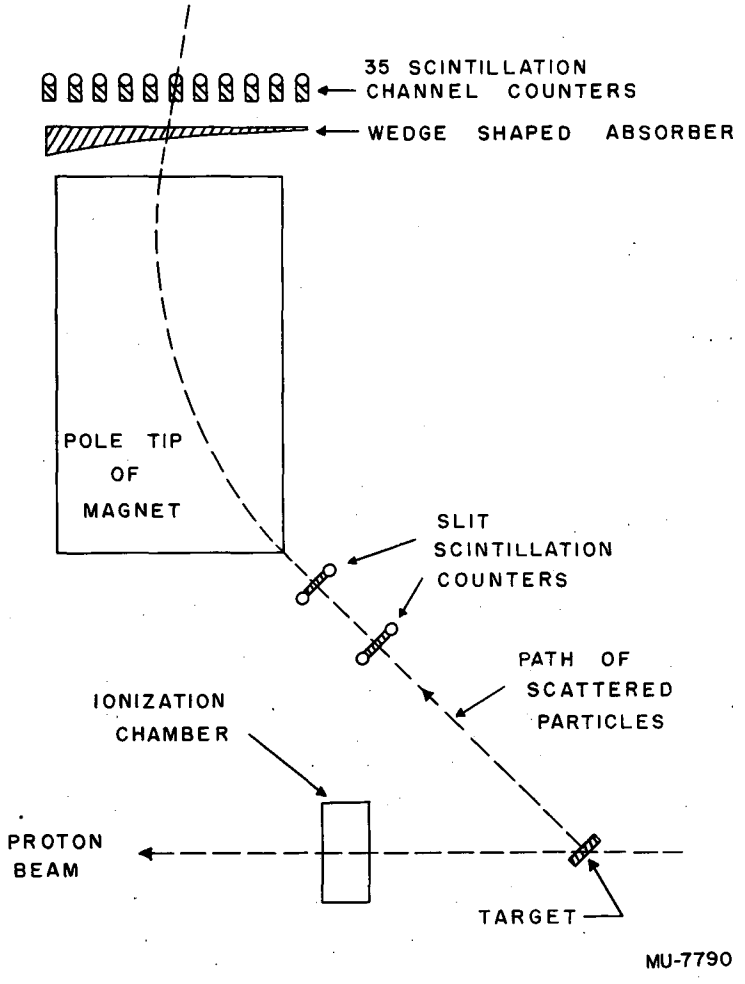

Fig. 8 Experimental Apparatus Used in the Hρ-Range Method

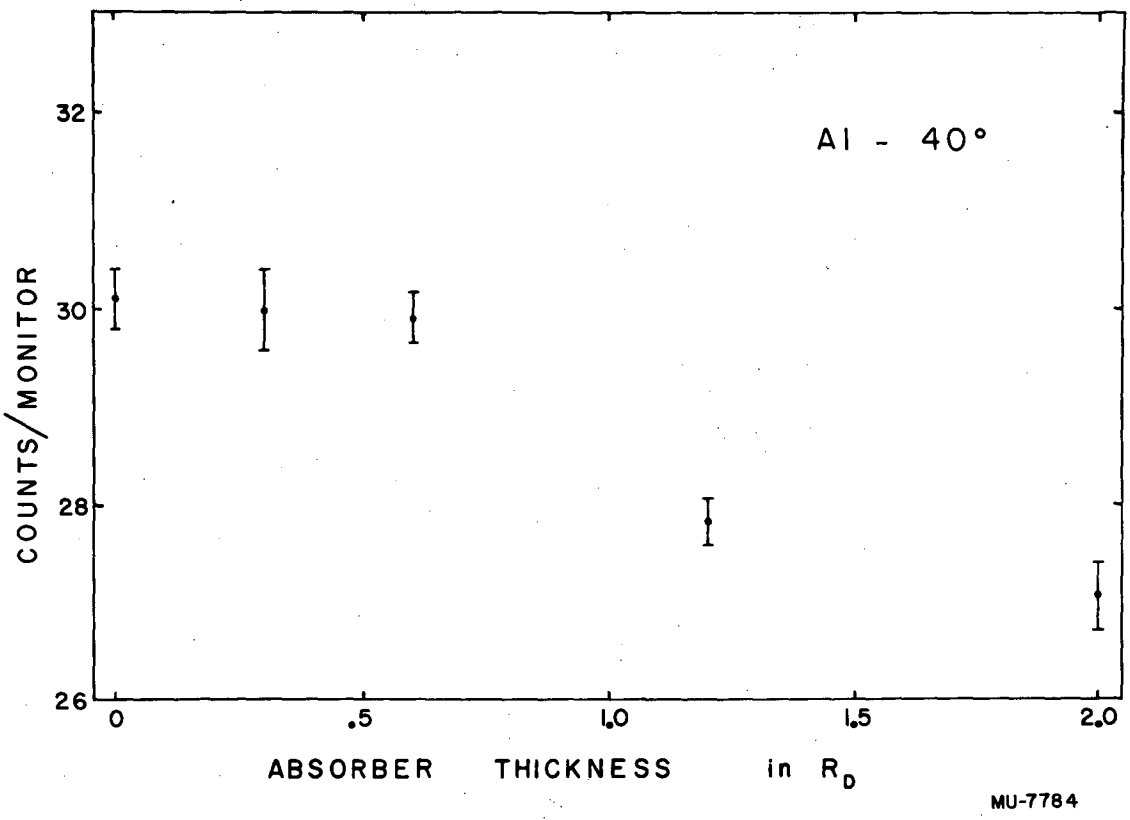

Fig. 9 An Absorber Curve Obtained Using the Hρ-Range Method.

The range ratios are essentially independent of the particle energy. The He^3 and He^4 have twice the momentum of the other particles for the same Hρ because they have Z = 2. From the table above one can see that it is easy to separate deuterons from protons and deuterons from tritons but that tritons and He^4 may be confused and slmost certainly deuterons and He^3 will be confused. From the absorber curve (Fig. 9) one can see that the yield of tritons + He^4 is unmeasurably small. It is reasonable to assume therefore that the contribution at $R_D = 1$ is due to deuterons and not to He^3. This is borne out by the E - dE/dx data. Although the separation of protons from deuterons is more complete here than when E - dE/dx is used this method has one big disadvantage. Individual events cannot be labeled as deuterons or protons. A subtraction involving two absorber thicknesses must be made and this makes the statistics worse, especially since the deuteron yield is only about 5 %, which means that the subtraction involves a small difference between two large numbers. This effect limited the use of the Hρ - range method to the proton beam experiments where the counting rates were reasonable. In the neutron beam the counting rates were too low to make this method useful.

The energies of the particle orbits through the magnet were determined by passing a current-carrying wire under tension through the field. This wire maps out the orbits and determines the particle momenta for the orbits by the relationship

$$\frac{\text{Tension in dynes}}{\text{Current in abamps}} = H\rho \text{ in gauss cm}$$

The orbits for the particles passing through the magnet were determined by the fact that they had to originate at the target, and then pass through two thin "slit" scintillation counters, and then having been deflected by the magnet strike one of the 35 channel scintillation counters.

Figure 10 is a block diagram of the electronics used in connection with the Hρ - range apparatus. The scattered particle passes through the two slit scintillation counters. The resulting light pulses are received by the 1P21 phototubes and the signals from the two tubes on each crystal added in a triode adder circuit similar to that shown in Figure 11. Also

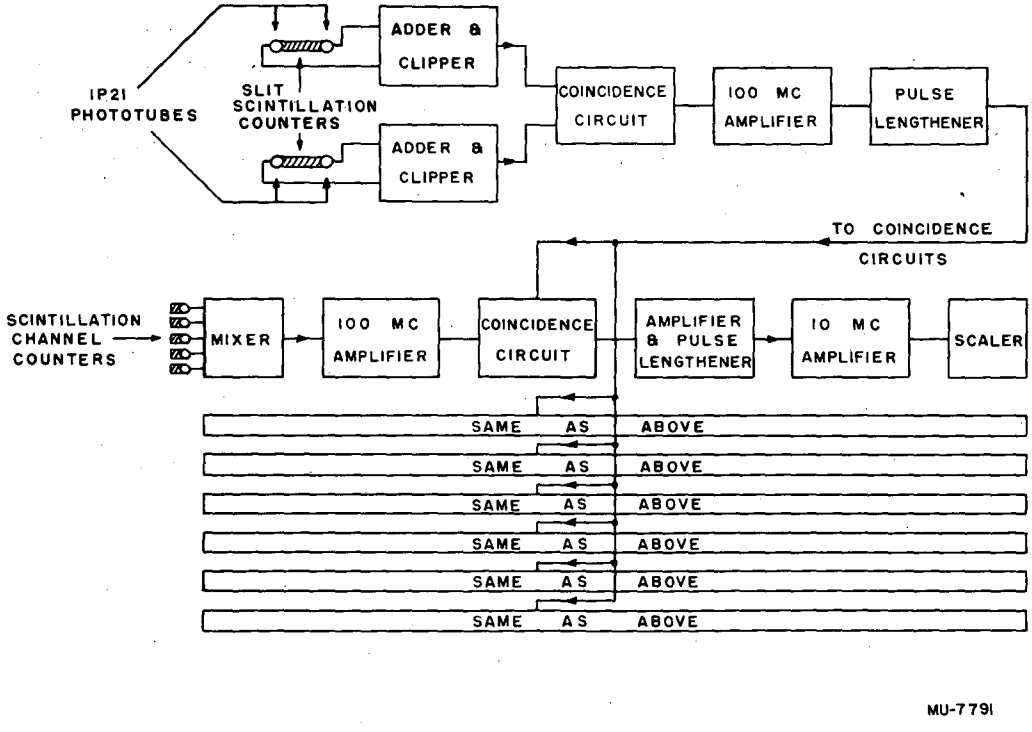

Fig. 10 Block Diagram of the Electronics Used with the Hρ-Range Method.

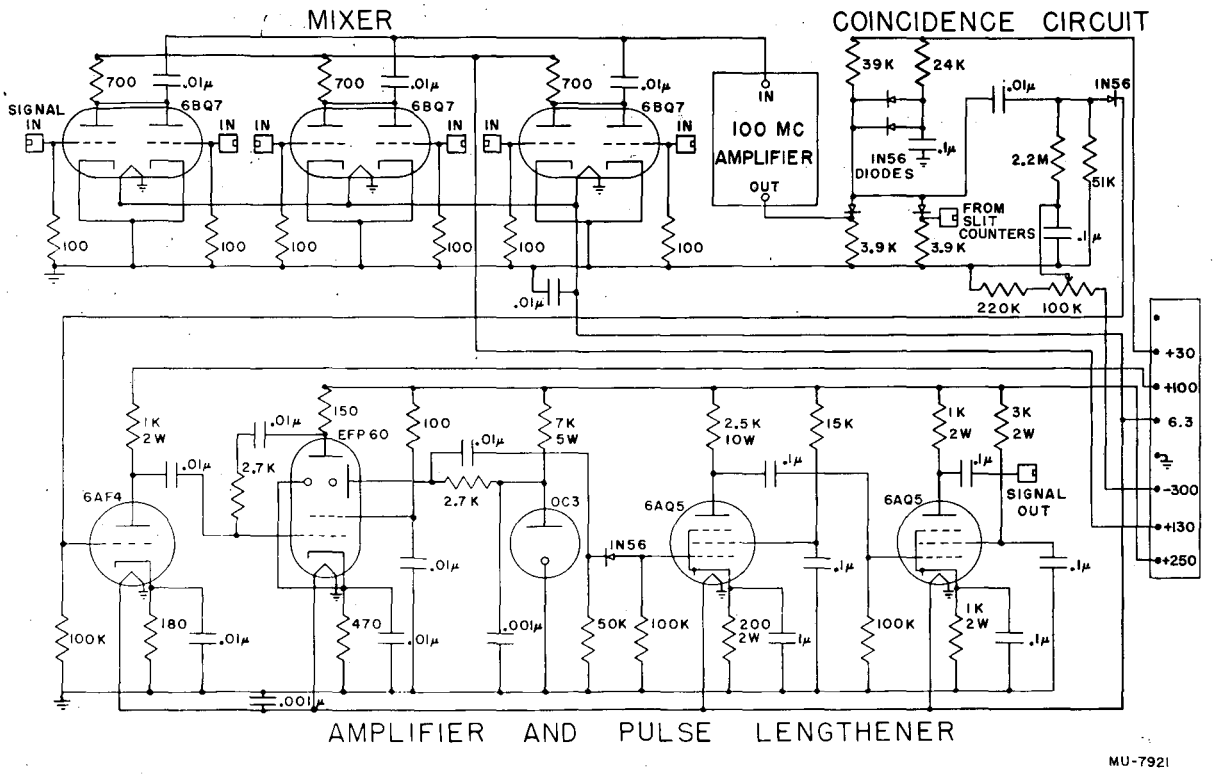

Fig. 11 Mixer - Coincidence Circuit and Amplifier Used in the Hρ-Range Method.

incorporated in the grid of this circuit is a section of cable of such a length that the pulse reflected along this line upon returning to the grid clips the original signal to a length of 5×10^{-9} sec. The length of these pulses determine the resolving time of the coincidence circuit into which the signals are fed. This is a germanium diode circuit similar to that shown in Fig. 11. The output of this circuit is amplified and lengthened and fed into seven coincidence circuits. The other input to these coincidence circuits comes from a mixer circuit in which five or six of the channel scintillator counter signals are mixed. Fig. 11 shows this mixer circuit, the coincidence circuit that follows it, and the succeeding amplifier. The mixing process makes the energy resolution worse but reduces the amount of electronics needed. A signal coming from one of the seven coincidence circuits indicates that a particle has gone through the two slit scintillation counters and then through one of the group of channel counters feeding the coincidence circuit under question. The outputs of the seven coincidence circuits are amplified and then scaled. The counting rates of these scalers as a function of absorber thickness determine the yields of the various scattered particles.

III. ANALYSIS OF DATA

A. E - dE/dx Method

1. General Method

Pulse height data were recorded on 35-mm film free running through a General Radio movie camera focused on the scope face. The beam level was adjusted so that about one sweep on the scope per inch of film was recorded. It was determined that the 12 kilovolt accelerating voltage on the scope gave enough intensity to photograph. This allowed larger signal deflections on the scope, up to four centimeters, before the amplifiers in the scope saturated. The film was developed and projected on a microfilm viewer and the pulse heights were read and plotted. A sample of the data taken with an Al target at 40^{o} is shown on Fig. 12. These data show clearly the proton line and also the deuteron line. Also less evident, but present, is a contribution of tritons. If the proton, deuteron and triton lines are drawn in on this plot as in Fig. 7, and lines of constant mass are then drawn between these three lines, a particle mass distribution curve can be obtained by counting the events lying between the various lines. A mass spectrum arrived at in this way is shown in Fig. 13. It is seen that the deuteron peak is quite well separated from the proton distribution, and also that there are some tritons present and that they are moderately well separated from the deuterons.

The counting rate of the scaler that was recording the number of scope traces was used to obtain the differential cross section for all scattered charged particles from target X, which is given by

$$\sigma_x(\theta) = \frac{C_x}{N_x n_x}\left(\frac{1}{\Omega \epsilon}\right) \qquad (1)$$

C_x = Scaler Counts
N_x = Corresponding monitor reading
n_x = Target atoms/cm^2
Ω = Solid angle
ϵ = Counting efficiency

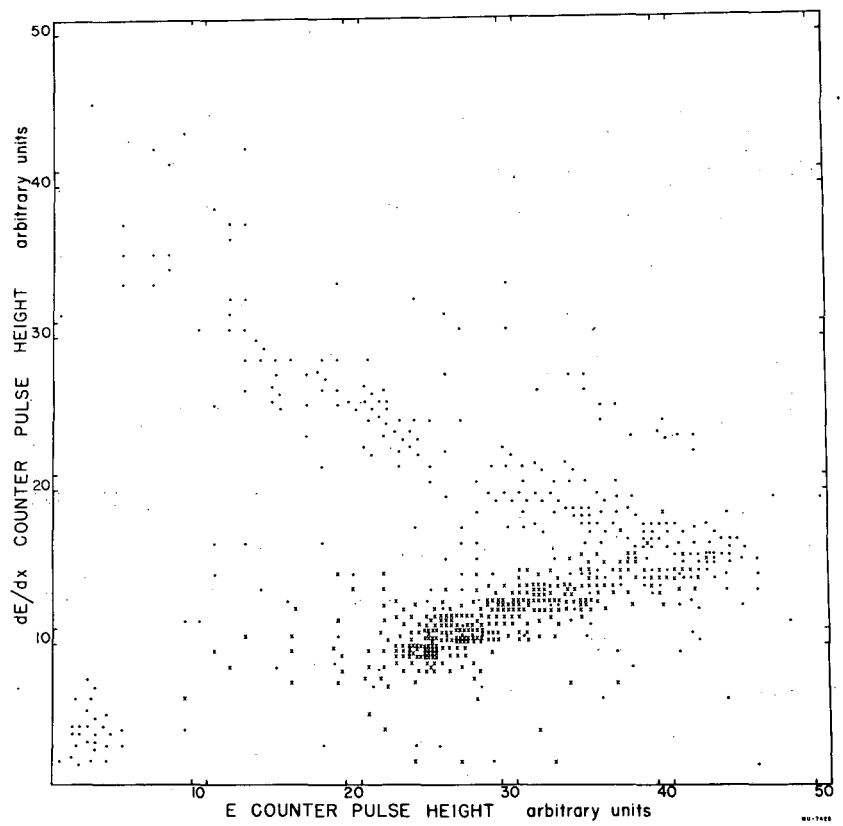

Fig. 12 A Sample of Data Taken Using the E- $\frac{dE}{dx}$ Method.

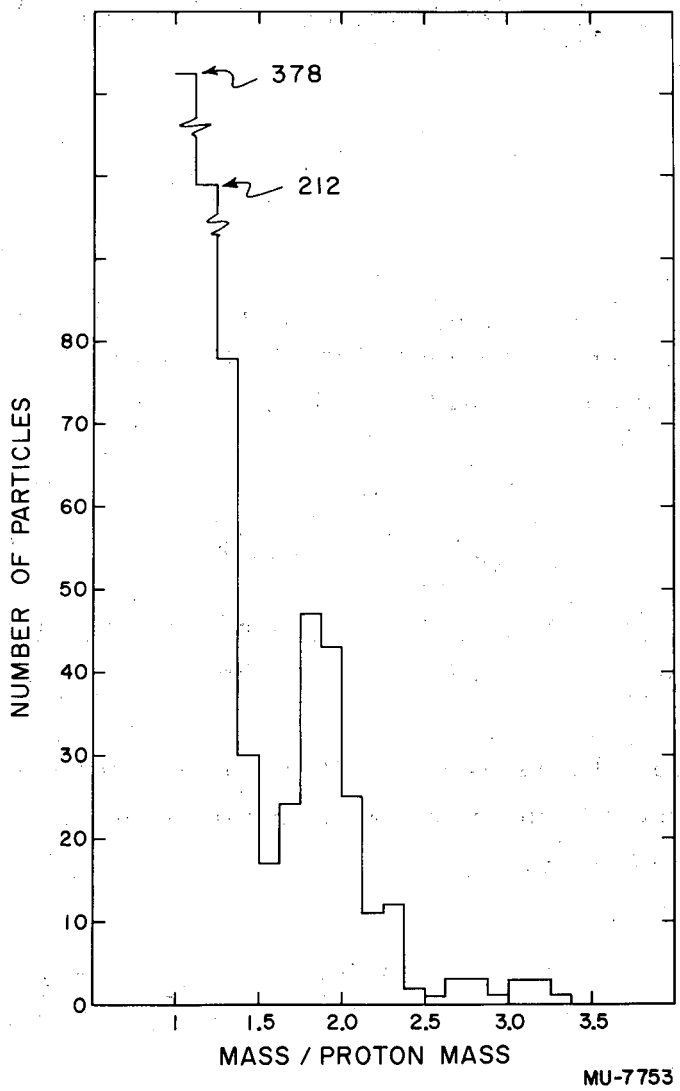

Fig. 13 Mass Spectrum Obtained from E- $\frac{dE}{dx}$ Data.

The produce $\Omega\epsilon$ is determined in a manner that makes the cross section in Eq. (1) absolute. This is done by using a CH_2 - C target difference and using the known free nucleon - nucleon cross sections.

$$\frac{C_{CH_2}}{N_{CH_2}} = \sigma_c(\theta) n_{C \text{ in } CH_2} \Omega\epsilon + \sigma_{\text{nucleon}}(\theta) n_{H \text{ in } CH_2} \Omega\epsilon \qquad (2)$$

$$\frac{C_C}{N_C} = \sigma_C(\theta) n_C \Omega\epsilon \qquad (3)$$

In the above $\sigma_{\text{nucleon}}(\theta)$ is $\sigma_{pp}(\theta)$ for an incident proton beam or $\sigma_{np}(\theta)$ for an incident neutron beam. The values used for these cross sections were,[11] in millibarns/steradian:

	cm		lab	
	$\sigma_{pp}(\phi)$	$\sigma_{np}(\phi)$	$\sigma_{pp}(\theta)$	$\sigma_{np}(\theta)$
26^o	3.4	2.80	13.6	11.2
40^o	3.7	1.75	11.6	5.45

The values taken from the literature are the center of mass values. The values used in the cross section determinations are the laboratory values, which are obtained by

$$\frac{\sigma(\vartheta)_{lab}}{\sigma(\phi)_{cm}} = \frac{d\Omega_{cm}}{d\Omega_{lab}} = \frac{d \cos \phi}{d \cos \vartheta} \qquad (4)$$

$$\frac{\sigma(\vartheta)}{\sigma(\phi)} = 4 \cos \vartheta \left[\frac{1 - \beta^2}{(1 - \beta^2 \cos^2 \theta)^2} \right] \qquad (5)$$

where the angles are related by

$$\tan \vartheta = \sqrt{1 - \beta^2} \frac{\sin \phi}{1 + \cos \phi} \qquad (6)$$

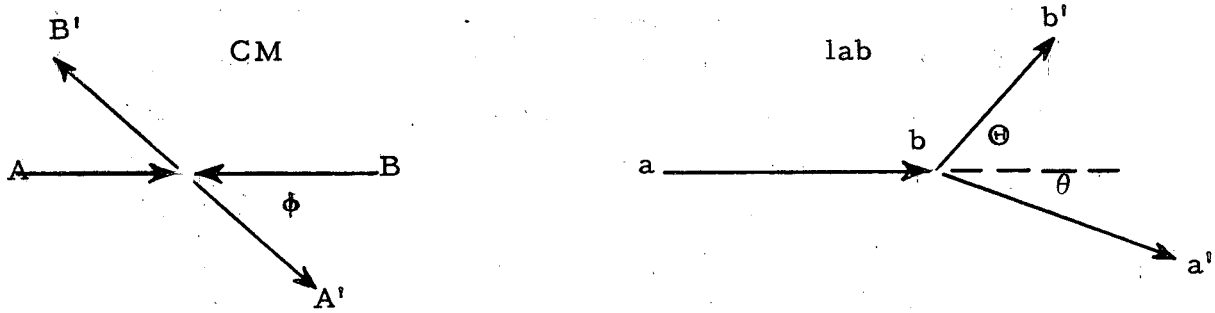

When one observes the struck particle after collision b' as in the n-p experiments, the above expressions must be changed to

$$\frac{\sigma(\Theta)}{\sigma(\phi)} = 4 \cos \Theta \left[\frac{1 - \beta^2}{(1 - \beta^2 \cos^2 \Theta)^2} \right] \tag{7}$$

$$\tan \Theta = \sqrt{1 - \beta^2} \, \frac{\sin \phi}{1 - \cos \phi} \tag{8}$$

The β in the above discussion is for the center of mass and is given by

$$\beta = \frac{\sqrt{E_1^{\,2} + 2E_1 E_2}}{E_1 + 2E_0} \tag{9}$$

where E_1 = kinetic energy of beam nucleon
E_0 = rest energy of nucleon

Eliminating $\sigma_C(\theta)$ from Eqs. (2) and (3), we get

$$\Omega \epsilon = \left[\frac{C_{CH_2}}{N_{CH_2}} - \frac{n_{C \text{ in } CH_2}}{n_C} \left(\frac{C_C}{N_C} \right) \right] \frac{1}{n_{H \text{ in } CH_2}} \frac{1}{\sigma_{\text{nucleon}}(\theta)} \tag{10}$$

This value of $\Omega \epsilon$ is used in Eq. (1).

The cross sections in equation (1) results from a combination of protons, deuterons, tritons and neutrons which make recoil protons. In order to get individual particle cross sections we return to the pulse height data. By superimposing proton-deuteron and deuteron-triton separation lines, which can be obtained from Fig. 6, onto the pulse height data as shown in Fig. 12 we can determine the fractions of the total counts that are protons, deuterons, and tritons. The target out yield must be subtracted away in order to get these fractions. Using these numbers we can get the cross sections for production of protons, deuterons, and tirtons from nucleons bombarding element X.

$$\sigma_{\text{nucleon} + x \to p}(\theta) = \sigma_x(\theta) \left[\frac{\text{Protons}}{\text{All Particles}}\right] \tag{11}$$

$$\sigma_{\text{nucleon} + x \to d}(\theta) = \sigma_x(\theta) \left[\frac{\text{Deuterons}}{\text{All Particles}}\right] \tag{12}$$

$$\sigma_{\text{nucleon} + x \to t}(\theta) = \sigma_x(\theta) \left[\frac{\text{Tritons}}{\text{All Particles}}\right] \tag{13}$$

The subscripts on the cross sections on the left above mean

Incident Beam Nucleon + Target x → Observed Scattered Particles

It must be remembered that only particles above certain cutoff energies are counted. The threshold energies are listed in the previous section. Tables I and II give a summary of the cross sections obtained in this way. Figure 14 shows the deuteron differential cross sections for proton bombardment of various elements at an angle of 40° to the beam. Figure 15 shows all the differential proton cross sections measured in the course of the experiment plotted against A. Figure 16 shows differential cross sections for triton production at 40° to a proton beam.

We can also obtain energy spectra from the pulse height data as shown in Fig. 12. Taking the results of the calibration run as shown in Fig. 7 and by using the calculated E - dE/dx lines as shown in Fig. 6, we can draw lines of known energy perpendicular to the E - dE/dx lines. By counting the number of events between two such lines and dividing by the energy interval we can get the energy spectra. This method is not

Table I

Differential Cross Sections Obtained Using 300 Mev Protons
(All Values are in millibarns/steradian)

	Lithium	Carbon	Aluminum	Copper
$\sigma_{p+x\to p}(26^\circ)$	---	70.0 ±4.0	130.1 ±5.0	188.5 ±7.0
$\sigma_{p+x\to p}(40^\circ)$	35.3 ±3.0	52.3 ±4.0	89.0 ±4.0	142.8 ±6.0
$\sigma_{p+x\to d}(26^\circ)$	---	1.72 ±0.41	3.54 ±0.75	6.44 ±1.32
$\sigma_{p+x\to d}(40^\circ)$	1.16 ±0.31	1.90 ±0.35	4.69 ±0.48	7.86 ±1.04
$\sigma_{p+x\to d}(60^\circ)$	---	1.42 ±0.30	---	---
$\sigma_{p+x\to t}(26^\circ)$	---	0.120±0.068	0.150±0.108	0.316±0.179
$\sigma_{p+x\to t}(40^\circ)$	0.079±0.042	0.148±0.069	0.415±0.108	0.260±0.189
$\sigma_{p+x\to t}(60^\circ)$	---	0.024±0.041	---	---

	Cadmium	Lead	Uranium
$\sigma_{p+x\to p}(26^\circ)$	---	290.0 ±12.0	---
$\sigma_{p+x\to p}(40^\circ)$	193.2 ±9.0	234.0 ±12.0	251.0 ±11.0
$\sigma_{p+x\to d}(26^\circ)$	---	13.9 ± 2.86	---
$\sigma_{p+x\to d}(40^\circ)$	11.22 ±1.20	18.0 ± 2.14	16.80 ± 1.68
$\sigma_{p+x\to d}(60^\circ)$	---	---	---
$\sigma_{p+x\to t}(26^\circ)$	---	1.22 ± 0.550	---
$\sigma_{p+x\to t}(40^\circ)$	0.492±0.296	2.035± 0.596	0.191± 0.248
$\sigma_{p+x\to t}(60^\circ)$	---	---	---

Table II

Differential Cross Sections Obtained Using 300 Mev Neutrons
(All Values are in millibarns/steradian)

	Lithium	Carbon	Aluminum	Copper
$\sigma_{n+x\to p}(26^\circ)$	---	27.7 ±2.0	49.2 ±3.0	76.3 ±5.0
$\sigma_{n+x\to p}(40^\circ)$	9.6 ±0.85	16.15 ±0.77	29.7 ±1.4	46.8 ±1.9
$\sigma_{n+x\to d}(26^\circ)$	---	2.80 ±0.40	4.15 ±0.50	7.08 ±0.86
$\sigma_{n+x\to d}(40^\circ)$	1.13 ±0.17	2.09 ±0.20	3.87 ±0.40	5.31 ±0.62
$\sigma_{n+x\to t}(26^\circ)$	---	0.311±0.133	0.860±0.195	0.715±0.295
$\sigma_{n+x\to t}(40^\circ)$	0.092±0.026	0.291±0.061	0.599±0.124	0.992±0.196

	Cadmium	Lead	Uranium
$\sigma_{n+x\to p}(26^\circ)$	---	120.2 ±9.0	---
$\sigma_{n+x\to p}(40^\circ)$	64.2 ±2.4	80.4 ±3.3	83.3 ±3.3
$\sigma_{n+x\to d}(26^\circ)$	---	9.71 ±1.60	---
$\sigma_{n+x\to d}(40^\circ)$	8.85 ±0.78	10.03 ±1.12	9.97 ±1.17
$\sigma_{n+x\to t}(26^\circ)$	---	1.60 ±0.61	---
$\sigma_{n+x\to t}(40^\circ)$	0.820±0.217	1.948±0.395	1.518±0.380

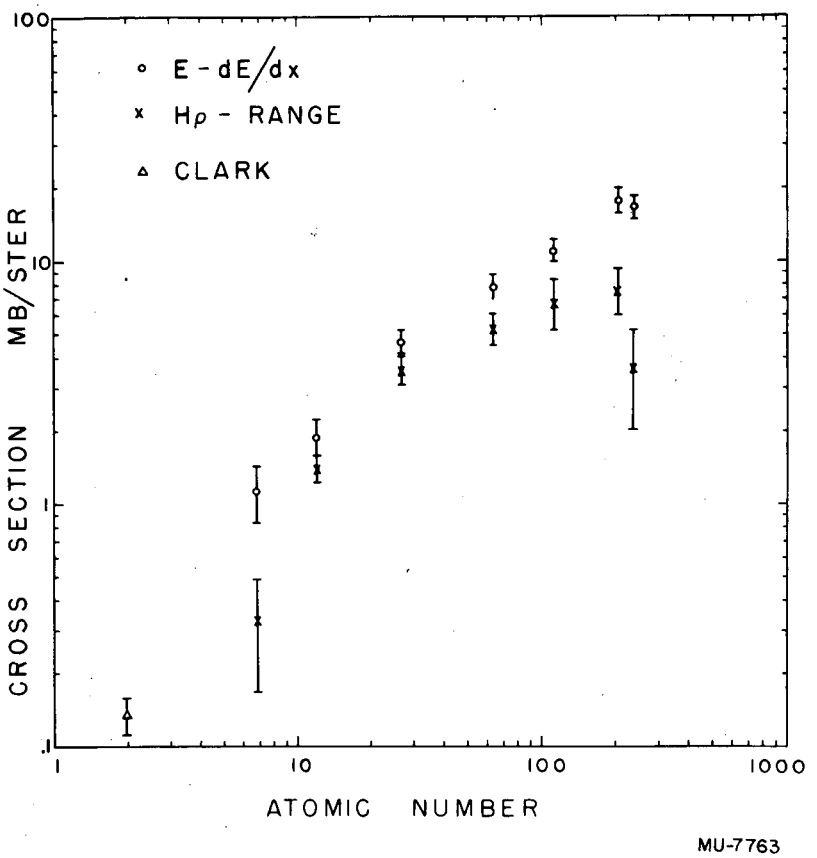

Fig. 14 Deuteron Differential Cross Sections at 40^{o}.

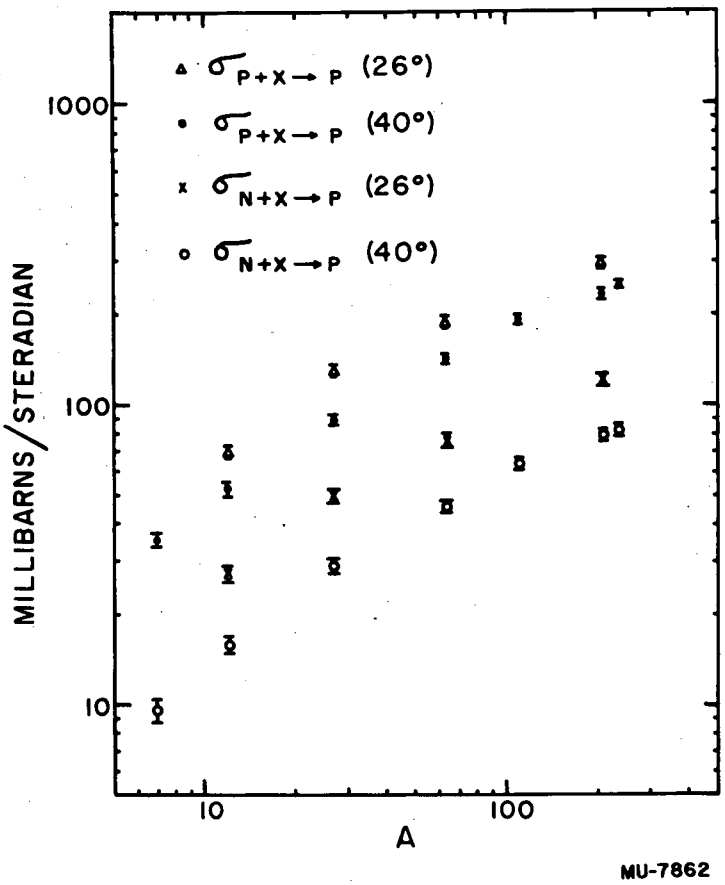

Fig. 15 Proton Differential Cross Sections.

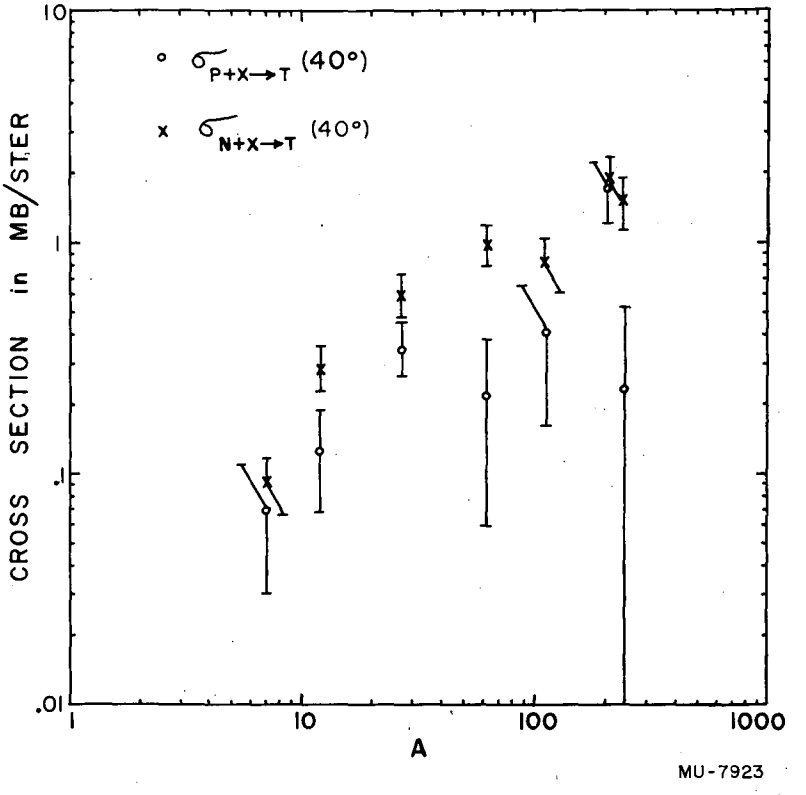

Fig. 16 Triton Differential Cross Sections at 40°.

as reliable as the Hρ - range method. Comparing proton energy spectra made by Hρ and range with those made by E and dE/dx showed that in each case the two lowest energy points made by E and dE/dx were low by the same amount. Since the E - dE/dx data were more probably in error rather than the Hρ - range data, these points have been raised on the proton energy spectra figures. Proton spectra obtained from the E - dE/dx data are shown in Figs. 17, 18, and 19. The Hρ - range data are not included since they were taken at 340 Mev rather than at 300 Mev. Comparison of E - dE/dx and Hρ - range proton spectra both made at 340 Mev agree well except for the two low energy points. There are several possible reasons why the E - dE/dx method may show low yields of low energy particles. First the particles having energy enough to just get into the E crystal will produce small light pulses there. Saturation of the light output near the end of the range[10] reduces the size of the light pulse. The magnitude of the saturation for the scintillators used is not known, but may be a large effect. This means that some light pulses may be too small to detect. Secondly the 1P21 phototubes used to produce the signal triggering the oscilloscope sweep circuit were not well located to observe low energy particles. These tubes were centered on the three-inch width of the crystal whereas the light pulse originates near the edge of the crystal. For example, a 10 Mev deuteron travels only about 1 mm into the plastic scintillation. This poor geometry would tend to make the light pulse seen by the phototube smaller. Lastly, the effects of multiple scattering and range straggling are more important for low energy particles and may decrease the number reaching the E crystal. A rough calculation shows that this should not be important except for particles leaving the dE/dx crystal with a few Mev or less.

All these effects tend to decrease the counting efficiency for the E - dE/dx method for low energy particles. There are no comparable difficulties in the Hρ - range technique so it is assumed the Hρ - range points are the correct ones.

Deuteron spectra made by E - dE/dx and Hρ - range methods for an angle of 40° are shown in Fig. 20. The two low energy points on the deuteron spectra obtained by E - dE/dx are also obviously too low, but it was difficult to make a direct comparison with Hρ - range deuteron

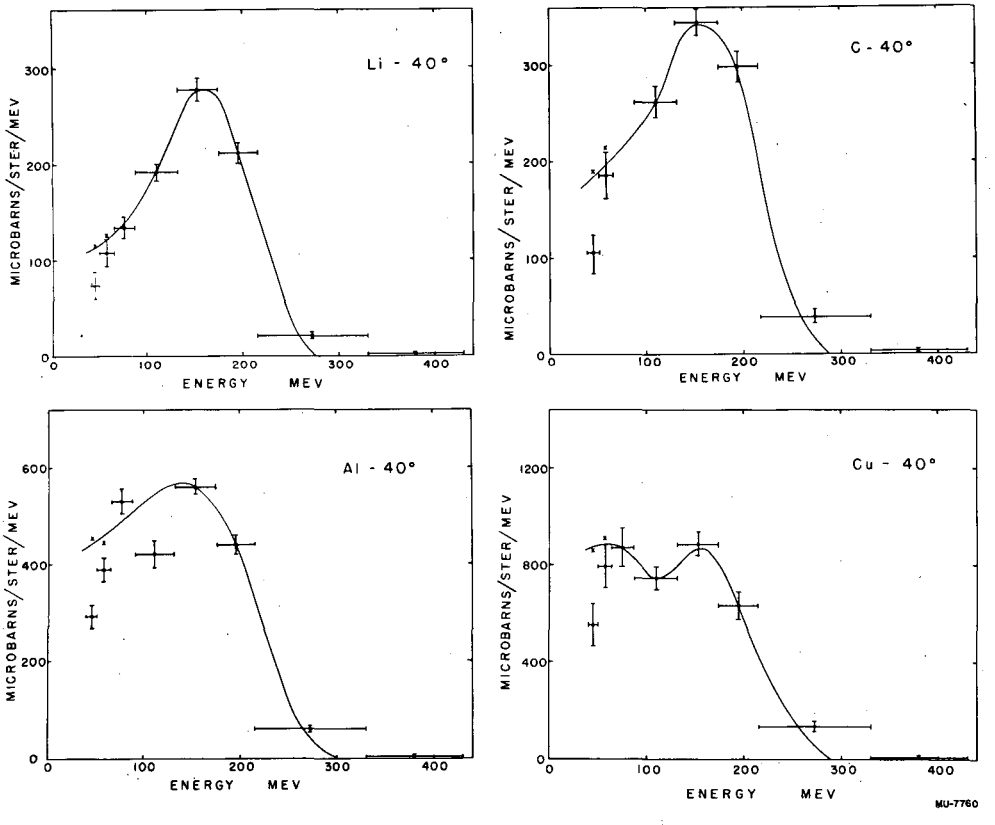

Fig. 17 Energy Spectra of Protons at 40° to the Beam for Various Elements Bombarded with 300 Mev Protons.

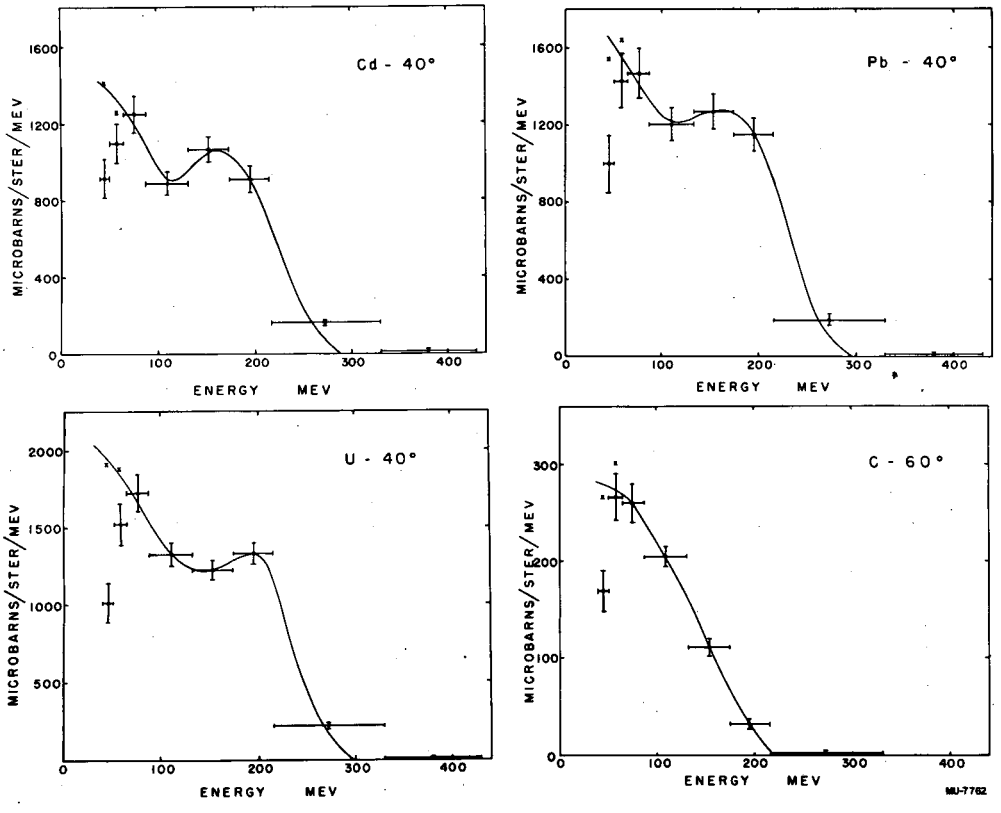

Fig. 18 Energy Spectra of Protons at 40° or 60° to the Beam for Various Elements Bombarded with 300 Mev Protons.

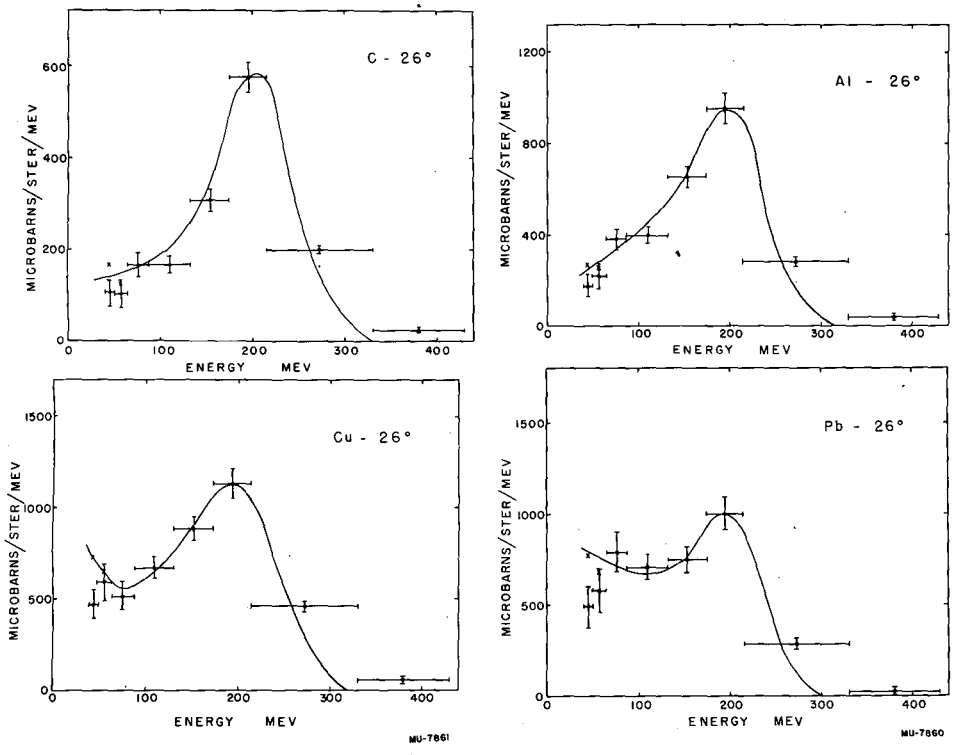

Fig. 19 Energy Spectra of Protons at 26° to the Beam for Various Elements Bombarded with 300 Mev Protons.

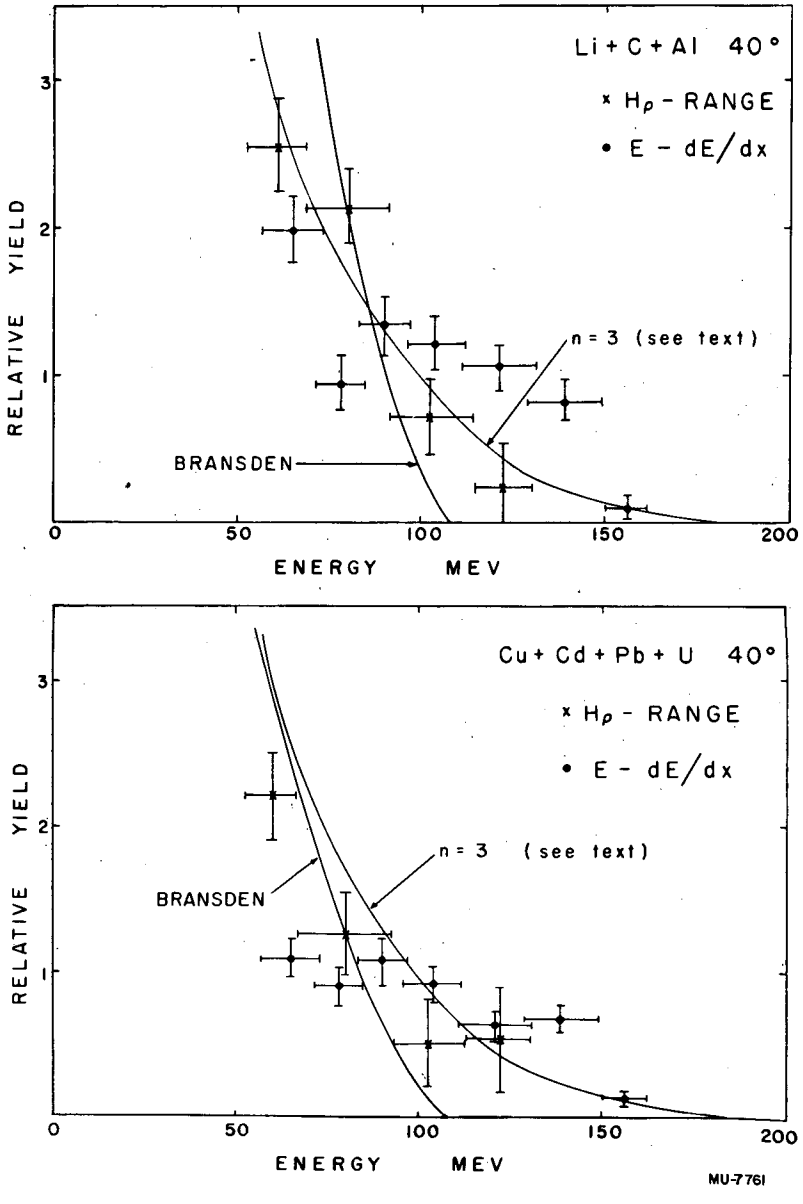

Fig. 20 Energy Spectra of Deuterons at 40° to the Beam for Light and Heavy Elements Bombarded with 300 Mev Protons.

spectra so no corrections were made in this case. Deuteron spectra made by E - dE/dx for angles of 26° and 60° are shown in Fig. 21.

Although the difference observed in the low energy part of the spectra found using the two experimental methods has not been carefully resolved, none of the essential conclusions drawn from the experiment is nullified.

B. Hρ - Range Information

The absorber curves such as in Fig. 9, obtained using the magnet, can be analyzed to get the differential cross sections for production of deuterons. The dip in the absorber curve at the deuteron range is quite apparent. The magnitude of this dip at $R_D = 1$ compared to the height of the curve for an absorber thickness of $R_D = 0$ gives the fraction of charged particles that are deuterons. The magnitude of this dip must be corrected for proton nuclear absorption in the wedge shaped absorbers. This can be done by using the rest of the absorber curve.

The cross section for producing deuterons is obtained in a manner similar to that used in the previous section. The cross section for all scattered charged particles is obtained from the counting rate C_x of the slit scintillation counters as was done before,

$$\sigma_x(\theta) = \frac{C_x}{N_x n_x}\left(\frac{1}{\Omega\epsilon}\right)$$

where $\Omega\epsilon$ is obtained in the way described. From this we can get the deuteron cross section by

$$\sigma_{p+x\rightarrow d}(\theta) = \sigma_x(\theta)\left[\frac{\text{Deuterons}}{\text{All Particles}}\right]\left(\frac{1}{M}\right) \qquad (14)$$

The factor M takes care of the fact that the magnetic particle spectrometer does not count all the scattered protons counted by the slit counters because of its high and low energy limits. M is determined by finding the fraction of the area under the proton energy spectra that the spectrometer does not count. The cross sections obtained this way using 340 Mev protons and a low energy cutoff for deuterons of 53 Mev are shown in Fig. 14.

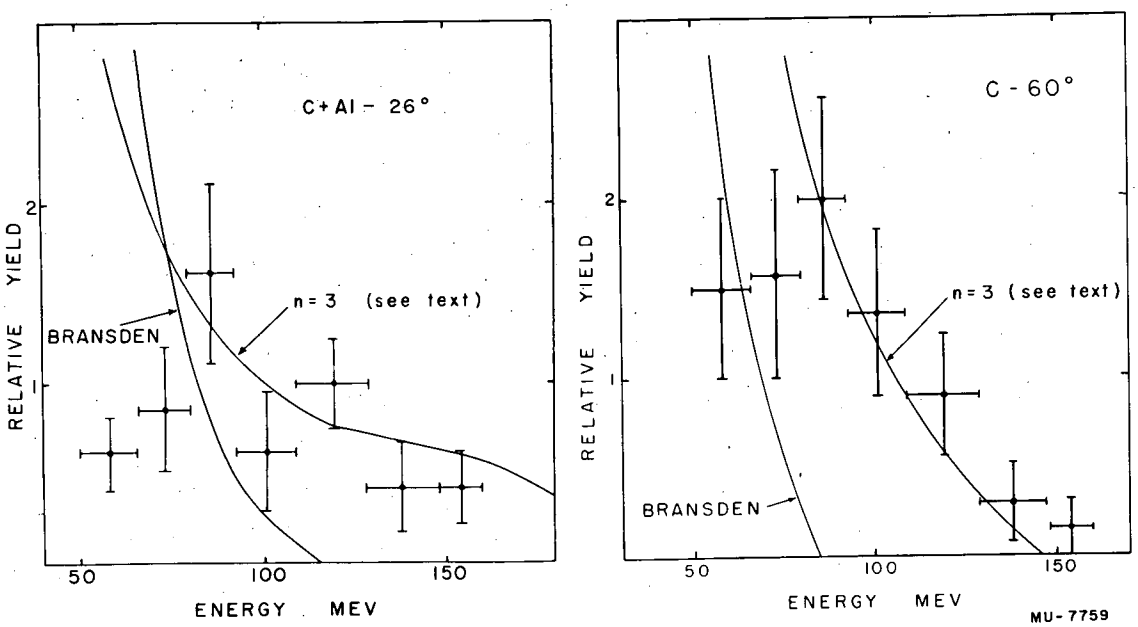

Fig. 21 Energy Spectra of Deuterons at 26° and 60° to the Beam when Light Elements are Bombarded with 300 Mev Protons.

Energy spectra are obtained from the Hρ - range data by taking the counting rate of one channel at a time instead of the total counting rate. The energy widths of the channels are determined by the current-carrying-wire orbit mapping technique. The deuteron energy spectra obtained using Hρ and range are shown in Fig. 20. Several elements have been combined to improve the statistics. The shapes of these spectra are more reliable than the spectra obtained using E and dE/dx because it is difficult to assign good energy values to positions along the E - dE/dx lines shown on Fig. 6.

C. Errors

The errors listed in Tables I and II contain more than counting statistics, so they should be explained.

1. The errors quoted in the proton differential cross section measurements are larger than statistical. One point that was considered besides counting statistics was the reproducibility from run to run of these cross sections. Also an error of about 3 % was allowed on the values of $\sigma_{pp}(\theta)$ and $\sigma_{np}(\theta)$ which were used in determining the absolute cross sections (see Table I).

2. The errors in the deuteron cross sections arise mainly from two sources. First, the standard deviation of the number of deuterons observed was used and then an allowance was made for the fact that the deuterons were not completely separated from the proton distribution (see Fig. 13). The pulse height data were inspected and the number of events that could have been either protons or deuterons was determined, and half of this number was taken as an error in the separation. This number was compounded with the error in the number of deuterons and also compounded with the error in the differential cross section for all particles = $\sigma_x(\theta)$. The result of this is considered to be the standard deviation of the deuteron cross sections. The same process was used to get the standard deviations in the triton differential cross sections.

3. The errors shown in all the energy spectra are just standard deviations of the number of events observed.

4. The errors shown in Fig. 25 are obtained by compounding the errors in the four cross sections used to obtain the values of x (see

Appendix I). Because of the way the cross section errors are obtained, the errors for x can be considered to be standard deviations.

IV. A CALCULATION OF DEUTERON YIELDS AND ENERGY SPECTRA

It seemed worth while to use the indirect pickup process model proposed for the deuteron formation mechanism and by starting with known spectra and yields of scattered protons, to try to fit the deuteron spectra and yields. Using this approach we write, for the carbon nucleus as an example, that the cross section for producing indirect pickup deuterons using an incident proton beam, is the product of the cross section for scattering the beam protons and the probability that a scattered nucleon picks up to form a deuteron. This gives us the following expression for the deuteron energy spectrum:

$$\frac{d\sigma_{p+c\rightarrow d}}{d\Omega\, dE} = \frac{d\sigma_{p+c\rightarrow p}}{d\Omega\, dE}(P_1) + \frac{d\sigma_{p+c\rightarrow n}}{d\Omega\, dE}(P_2) \qquad (15)$$

The first te rm on the right above is the contribution from scattered protons picking up neutrons. The second term is due to standard neutrons picking up protons. P_1 is the probability for a scattered proton to pick up a neutron to form a deuteron and P_2 is the probability for a scattered neutron to pick up a proton. In the course of this experiment we have measured

$$\frac{d\sigma_{p+c\rightarrow p}}{d\Omega\, dE} \text{ and } \frac{d\sigma_{p+c\rightarrow d}}{d\Omega\, dE}, \text{ but not } \frac{d\sigma_{p+c\rightarrow n}}{d\Omega\, dE}$$

For the shape of the scattered nuetron energy spectrum,

$$\frac{d\sigma_{p+c\rightarrow n}}{d\Omega\, dE},$$

the best guess is to take the shape of the measured proton spectrum,

$$\frac{d\sigma_{p+c\rightarrow p}}{d\Omega\, dE}$$

and change it point by point by the ratio of the free nucleon cross sections,

$$\frac{\sigma_{np}(\theta)}{\sigma_{pp}(\theta)}$$

Actually,

$$\frac{d\sigma_{p+c\to n}}{d\Omega\, dE} \approx \frac{d\sigma_{n+c\to p}}{d\Omega\, dE}, \tag{16}$$

where we have measured the energy spectrum on the right above, but the neutron beam energy spread is so large that this spectrum should not be compared with a spectrum obtained from a monoenergetic proton beam experiment.

The area under the spectra,

$$\frac{d\sigma_{p+c\to p}}{d\Omega\, dE} \text{ and } \frac{d\sigma_{p+c\to n}}{d\Omega\, dE}$$

were made equal to the measured differential cross sections,

$$\sigma_{p+c\to p}(\theta) \text{ and } \sigma_{n+c\to p}(\theta)$$

In this way we now know all the spectra involved in Eq. 15. The probability that a proton picks up a neutron P_1, should equal the probability that a neutron pciks up a proton P_2 for carbon, since the matrix element entering into both probabilities should be the same and the number of neutrons is the same as the number of protons in the carbon nucleus.

Using this information and, assuming that the energy dependence of the pickup probability can be written as a power law, we write

$$P_1 = P_2 = k\, E^{-n} \tag{17}$$

then taking a value for n and multiplying the two spectra,

$$\frac{d\sigma_{p+c\rightarrow p}}{d\Omega\, dE} \text{ and } \frac{d\sigma_{p+c\rightarrow n}}{d\Omega\, dE}$$

by E^{-n} and adding, we should get the deuteron energy spectrum. However, the energy scale must be corrected. The deuteron made by pick-up does not have the same energy as the scattered nucleon that produced the deuteron. When direct pickup takes place in deuterium we have non-relativistically,

$$E_{\text{Deuteron}} = \frac{8}{9} E_o \cos^2\theta \tag{18}$$

where E_o is the energy of the beam particle.

For a more complicated nucleus than deuterium, where there is not a two-body reaction, this relation does not hold exactly. In a complex nucleus the picked up nucleon can have more internal momentum than in deuterium, and the residual nucleus functions in an unknown manner in absorbing the recoil momentum. Also, the deuteron energy is decreased by the fact that the picked up nucleon binding energy (BE) must be supplied. We may write as an approximation for the energy relation in a complex nucleus

$$E_{\text{Deuteron}} = \frac{8}{9} E_o \cos^2\theta - BE \tag{19}$$

The retention of the coefficient $\frac{8}{9}$ here cannot be justified, but this coefficient must be near unity and the procedure used seems the most reasonable. Changing this coefficient would result in a change in BE. The value of BE can be evaluated from the data of Hadley and York.[2] Chew and Goldberger[3] pointed out that the 0^o deuteron spectrum from carbon of Hadley and York looked similar to the 90 Mev neutron spectrum but displaced to a 65 Mev peak; this gives

$$E_{\text{Deuteron}} = \frac{8}{9} E_o - BE = \frac{8}{9}(87) - BE = 65, \tag{20}$$

$$BE = 13 \text{ Mev}$$

Using this same value we can get the resultant deuteron energy spectrum taking $\cos^2\theta = 1$ as Chew and Goldberger did. Therefore we estimate the deuteron energy from the scattered nucleon energy by means of

$$E_{Deuteron} = \frac{8}{9} E_1 - 13 \qquad (21)$$

where E_1 is the energy of the scattered nucleon just before pickup occurs. A very similar result was obtained by Selove[12] studying pickup deuterons made from 95 Mev protons. Calculating BE from his data we obtain a somewhat lower value but changing the value used for BE does not change the results of the calculations appreciably. Curves constructed in the method outlined above using n = 1, 2, 3, 4, and 6 are shown in Fig. 22 with the corresponding experimental deuterium spectra superimposed on them. The areas under these curves above 50 Mev have been measured and are listed in Table III. The last column in the table lists the values used for the pickup probability,

$$P = kE^{-n}$$

which have been found by making the sum of the experimentally measured differential cross sections for deuteron production at the three angles used agree with the sum of the same cross sections as found by the method given in this section. These values of k were not used in plotting the deuteron energy spectra because of the uncertainty in the low energy part of the various spectra. Instead, all the curves were fitted to the experimental points at an energy of 75 Mev.

We are now in a position to decide which value of n gives the best results. First, looking at the differential cross sections, we can see that for n = 1 the differential cross section at 26° is quite high, and at 60° is quite low. For n = 6 this situation is reversed and for n = 4 the same is true as for n = 6 except to a lesser degree. The best fit is obtained by E^{-2} with E^{-3} a second choice.

Looking at the deuteron energy spectra, we see that in the spectra at all three angles, the E^{-1} curve seems to have too high an energy cutoff and the E^{-6} too low a cutoff. In addition, the E^{-6} curves seem to be

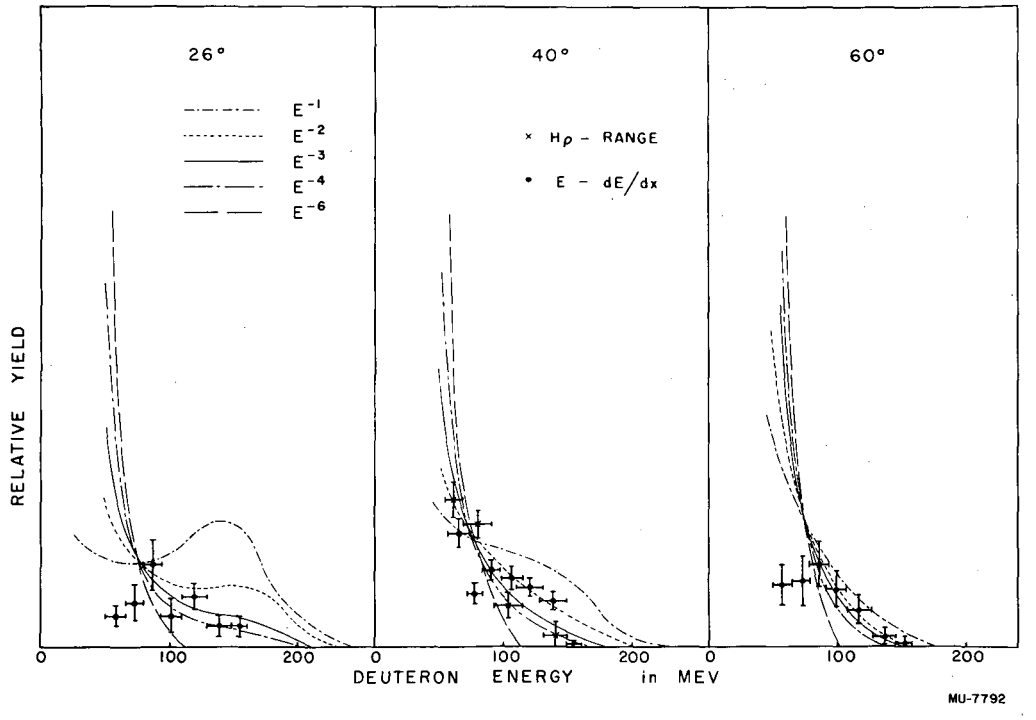

Fig. 22 Deuteron Energy Spectra Calculated by Using the Indirect Pick up Process and Assuming the Energy Depence of the Pick up Process to be given by E^{-n}. Values of n of 1, 2, 3, 4 and 6 were Used in the Calculation.

Table III

Angle to beam		26°	40°	60°	Expression Used For Pickup Probability
Measured Value		1.78 ± 0.41	1.90 ± 0.35	1.42 ± 0.30	---
Calculated Using	E^{-1}	2.39	1.61	1.19	$0.093 \left(\frac{E}{100}\right)^{-1}$
	E^{-2}	1.88	1.68	1.63	$0.115 \left(\frac{E}{100}\right)^{-2}$
	E^{-3}	1.69	1.70	1.80	$0.138 \left(\frac{E}{100}\right)^{-3}$
	E^{-4}	1.53	1.72	1.94	$0.138 \left(\frac{E}{100}\right)^{-4}$
	E^{-6}	1.26	1.70	2.23	$0.122 \left(\frac{E}{100}\right)^{-6}$

All cross sections given in millibarns/steradian.

All energies given in Mev.

too high at low deuteron energies. The 26° spectrum seems to indicate that the n = 2 curve contains too many high energy deuterons. The best fit here seems to be the E^{-3} or E^{-4} curve. It should be remembered that the two lowest energy E - dE/dx spectral points are believed to be abnormally low. This seemed to be the case with the proton spectra where the E - dE/dx data could be compared with the Hρ - range data.

On the basis of this analysis it appears that the energy dependence of the pickup probability is best given by E^{-2} or E^{-3}.

There have been other estimates of this energy dependence of the pickup process. Heidmann,[13] using the Born approximation, obtained a value of n = 6. Because of the nature of the Born approximation, this value is expected to be too high. Bratenahl,[14] using deuterium for the target nucleus, has obtained a value of $n \approx 3$ experimentally. Slater,[15] at this laboratory, in studying (d, p) reactions which are the inverse of the pickup process, found an energy dependence which for energies higher than 50 Mev can be written

$$\sigma = k E^{n} \tag{22}$$

where n is about 2.0 for several heavy elements. This should be closely related to the energy dependence of the pickup process.

Dr. Warren Heckrotte has pointed out that in the analysis by Chew and Goldberger[3] the cross section obtained has roughly an E^{-2} energy dependence. This can be seen from the fact that the matric element in the cross section is given by

$$\sum_{f} |H_f|^2 = \left[N(K - k) \right] \left[B_D + \frac{\hbar^2}{M} \left| k - \frac{K}{2} \right|^2 \right] \left[\left| \phi(r), \; e^{i(k - \frac{K}{2}) \cdot r} \right|^2 \right] \tag{23}$$

According to Chew and Goldberger the energy dependence in the second and third factors on the right cancel each other quite completely so that the energy dependence is given by N(K - k) which is the momentum distribution in the target nucleus. Taking Chew Goldberger momentum distribution

$$N(K - k) = \frac{1}{(E + 18)^2} \tag{24}$$

leads to an energy dependence of roughly E^{-2} for the energy region under consideration.

V. RESULTS AND CONCLUSIONS

A. Dependence of Proton Cross Sections on A

The differential cross section for scattering protons from light elements at 40° to the 300-Mev proton beam can be written as

$$\sigma_{p+x\rightarrow p}(40^{\circ}) = k_1 A^{n_1} \tag{25}$$

This results from the fact that the curves of Fig. 15 are fairly straight lines. Performing a least squares fit to this data for light elements leads to a value of $n_1 = 0.70$. Also, the cross section for scattered protons from neutron bombardments can be written

$$\sigma_{n+x\rightarrow p}(40^{\circ}) = k_2 A^{n_2} \tag{26}$$

The value of n_2 is 0.74.

The opaque nucleus model would predict an exponent of two-thirds for inelastic scattering but at this energy the semitransparent nucleus theory is more applicable. Dr. Warren Heckrotte predicted a value of $n = 0.78$ on the basis of the semitransparent nucleus theory.[16] A recent measurement of proton nuclear absorption cross sections[17] gave an exponent of $n = 0.73$. The values obtained in the present experiment would seem to agree with the predictions of the semitransparent nucleus theory. Other investigators have found comparable power laws for high energy nucleon inelastic scattering.[18]

B. Proton Energy Spectra

Proton energy spectra are shown for various elements at various angles in Fig. 17, 18, and 19. The spectrum from carbon at 40° compares well with Cladis's curve[5] for the same spectrum. The variation with A is what one would expect. The quasi-elastic peak stays visible all the way to Uranium, but the background of multiple collision events gets larger with A. The reason for this is that as the nucleus gets larger and probability for having more than one collision in the nucleus goes up. From the analysis of Wolff[6] we get

$$\frac{\text{probability of multiple collision}}{\text{probability of single collision}} = \frac{1 - e^{-\frac{4R}{3\lambda}} - \frac{4R}{3\lambda} e^{-\frac{4R}{3\lambda}}}{\frac{4R}{3\lambda} e^{-\frac{4R}{3\lambda}}} \qquad (27)$$

R = radius of nucleus under consideration

λ = mean free path in nuclear matter

This is the ratio of the number of events in which the incident particle collides with more than one target nucleon to the number of events in which the incident particles collide with a single nucleon in the target nucleus. The number of observed protons which originate in the multiple collision events might be three or four times as large as the number of events if all of the protons involved have enough energy to escape from the target nucleus. Similarly the number of observed protons from single collision events might be as large as twice the number of events because two nucleons are involved in each event. Monte Carlo calculations of collision events inside nuclei should be able to predict the number of observed particles for a particular type of event. Lacking this information the best we can do is to give a rough number for the ratio of observed protons thought to originate in single collision events. For uranium (see Fig. 18c) this is about five. This number is obtained by estimating the fraction of the total area under the energy spectrum which is due to quasi-elastic collisions. From Cladis's proton spectrum[5] from carbon at 40° it appears that a 1:1 ratio of single to multiple collisions fits his data.

The energy spectra for carbon at the various angles agree qualitatively with the spectra of Cladis and Temmer.[19]

C. Dependence of Deuteron Cross Sections on A

The differential cross section for deuteron production from light elements (lithium, carbon, and aluminum) at 40° to an incident proton can be written as

$$\sigma_{p+x\rightarrow d}(40^\circ) = k_1 A^{1.3} \quad H\rho \text{ - range data} \qquad (28)$$

$$\sigma_{p+x\rightarrow d}(40^{o}) = k_2 A^{1.1} \qquad E - \frac{dE}{dx} \text{ data} \tag{29}$$

An average value for the exponent is n = 1.2. This strongly suggests that the mechanism that produces these deuterons is the indirect pickup process described by Bransden.[4] A first guess for the value of the exponent of A based on this theory would be n = 2.0. This follows from the fact that the process is considered to be composed of two interactions, first a scattering of the initial nucleon and secondly a pickup process; each of these should go as A. The cross section which is the produce therefore should go as A^2. But it has been shown in this experiment that the differential cross section for nucleon scattering goes as $A^{0.72}$. Also, the A dependence of the direct pickup process is known. Using the total cross sections measured by Hadley and York[2] for making direct pickup deuterons from carbon and copper, one gets n = 0.41. The differential cross sections in the forward direction give a smaller number. Now, returning to the indirect pickup deuterons,

$$\sigma_{\text{indirect pickup}} = \left[\sigma_{\text{nucleon scattering}}\right] \left[\begin{matrix}\text{Pickup} \\ \text{Probability}\end{matrix}\right] \tag{30}$$

$$= \left[c_1 A^{.72}\right] \left[c_2 A^{.41}\right] = c_1 c_2 A^{1.13}$$

The exponent here agrees very well with those mentioned above, substantiating the theory of the indirect pickup process. It should be noted that the A dependence of the pickup part of the indirect pickup process implies that the pickup occurs on the surface of the nucleus. That is, the exponent n = 0.41 shows that as the target nucleus gets bigger only part of the added nucleons are important in producing the pickup deuterons. Since the mean free path of deuterons in nuclear matter is small compared to nuclear dimensions the important nucleons are the surface nucleons.

Chew and Goldberger, analyzing the data of Hadley and York, arrived at a similar conclusion:

> "Bombardments of copper and lead targets show that the number of fast deuterons increases with atomic number less rapidly than the number of fast protons.

This may be an indication that the pickup process is more confined to the surface of the nucleus than is a knock-out process."

It is interesting to note that the elastic P - D differential cross section measured by Clark[20] falls on this curve (Fig. 14) quite well. Actually, the cross sections for elements heavier than deuterium should be somewhat larger owing to the energy cutoff of the detecting apparatus. The fact that the elastic P - D cross section lies close to this line may imply that even in deuterium the two-step indirect pickup takes place. Bransden used in his calculation[4] something like a deuteron wave function for the two target nucleons involved in the event and treated the rest of the target nucleus in such a way that it entered into the event only through the conservation of energy equation. If this model were altered slightly it would predict that indirect pickup deuterons would be formed using a deuterium target as well as from more complex nuclei.

Copper and heavier elements do not obey the same A dependence as the light elements. The value of n here is about n = 0.6. There are several processes which might make the value of n different for light and heavy elements.

First, Serber stripping[21] should not be important here since the deuterons are made at or near the nuclear surface and there are essentially no nucleons along the path as the deuteron leaves the nucleus to cause this stripping.

Secondly, electric field stripping[22] may be responsible. One might write

$$\sigma_{\substack{\text{Indirect}\\ \text{pickup}}} = \left[\sigma_{\substack{\text{Nucleon}\\ \text{scattering}}}\right] \left[\begin{matrix}\text{Pickup}\\ \text{probability}\end{matrix}\right] \left[1 - \begin{matrix}\text{Stripping}\\ \text{probability}\end{matrix}\right] \qquad (31)$$

If we take the stripping probability = $0.0077\ Z^2$ we can fit the whole A dependence curve well. This is quite similar to the expression Dancoff derived. An analysis of the electric field stripping resulting when a deuteron starts inside a nucleus and moves outwards through the potential barrier has recently been made by Stuart.[23] This is the situation encountered in the present experiment. He showed that in this case the

electric field stripping is a small effect and that it varies more nearly like Z than Z^2. On the basis of Stuart's analysis we must assume that electric field stripping is not responsible for the heavy element cross section A dependence.

The third effect, which seems the most reasonable explanation has to do with the pickup probability. It has been demonstrated that the pickup takes place on the surface of the nucleus. The area of the surface that can be effective in the pickup process is limited by the fact that a deuteron cannot be formed if the two nucleons involved are farther apart than they can be in a deuteron. A measure of the separation in a deuteron is

$$\frac{1}{a} = \frac{\hbar}{\sqrt{m\epsilon}} = 4.8 \times 10^{-13} \text{ cm} \qquad (32)$$

An estimate of the area in which pickup could take place then could be a region roughly 4.8×10^{-13} cm in diameter centered on the point of exit of the scattered nucleon. Outside this area the surface nucleons would find it hard to make a bound state of a deuteron with a scattered nucleon. The radius of a copper nucleus is about

$$R_{cu} = 1.4 \times 10^{-13} (63.5)^{\frac{1}{3}} = 5.6 \times 10^{-13} \text{ cm} \qquad (33)$$

On this basis it is not surprising that for nuclei larger than copper the additional surface area is not effective in producing deuterons, and that as a result the pickup part of an indirect pickup process for heavy elements has an A dependence given by n = 0. Selove[12] has found that the direct pickup differential cross sections at 18° for making deuterons from copper and lead are essentially equal, also indicating that n = 0 for this case. This argument says that the fraction of scattered nucleons which pick up surface nucleons to form deuterons is independent of the target used for elements heavier than copper. But for lighter elements the fraction increases as the target nucleus gets lighter because a larger fraction of the surface nucleons are close to the scattered nucleon and therefore can be picked up more readily to form deuterons. As a result of this argument,

all the A dependence of the indirect pickup process for heavy elements is given by the nucleon scattering A dependence which for heavy nuclei is about n = 0.5 (see Fig. 15).

D. Deuteron Angular Distribution and Energy Spectra

Figure 23 shows the angular distribution of deuterons from proton bombardment of carbon. On the figure are the theoretical curve of Bransden and the curve obtained in Section IV of this report by using n = 3. The angular distribution is seen to be quite flat over the angular interval measured. The Born approximation curve of Bransden* is normalized to a total cross section in carbon of 9 millibarns. To make the curve fit at wide angles this total cross section would have to be increased considerably. Also the Bransden curve changes in height by a factor of 25 from 26° to 60°, while the experimental curve stays essentially flat. The curve claculated using n = 3 fits the data well. It should be remembered that the height of this curve has been fitted to the experimental data by choosing the value of k in $P = kE^{-n}$. The variation in height from angle to angle of the n = 3 curve is its important feature. It is seen to be essentially flat. This can be understood by considering that as the scattered proton yield decreases as we go to larger angles the spectrum of protons shifts to lower energies so that multiplying the proton spectrum by E^{-3} just compensates for the decreased yield. On this basis the deuteron angular distribution at angles smaller than 26° may be expected to be quite flat also.

The angular distribution claculated by Bransden may be too strongly peaked forward as a result of the initial wave function used in the calculation. The two nucleons to be interacted with within the nucleus were represented by a modified deuteron wave function. The assumption that the two target nucleons are related would lend a coherence to the process that probably is not present physically. This might produce a forward peaking.

---

*The author is deeply indebted to Dr. B. H. Bransden and Mr. J. McKee of Queens University, Belfast, Ireland, for extending the calculations of reference 3 to obtain the energy spectra and angular distribution of deuterons shown in Figs. 20, 21 and 23.

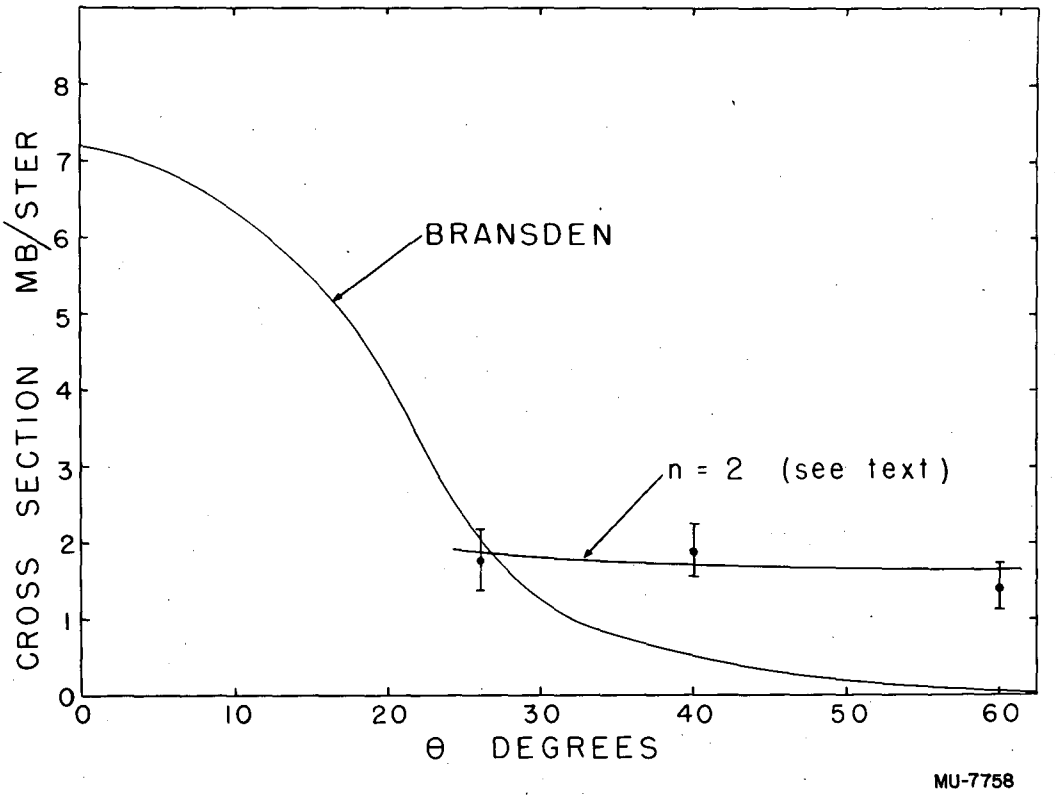

Fig. 23 Angular Distribution of Deuterons.

The deuteron energy spectra are shown in Fig. 20 and Fig. 21. The energy spectra calculated by Bransden and by the method of Section IV are shown on these figures.

The rough agreement of all the theoretical curves with the experimental data is evident. It should be remembered that the two lowest energy E - $\frac{dE}{dx}$ points are too low. The Bransden spectra seem to have somewhat too low an energy cutoff. It is noted that the 45° deuteron energy spectrum of Hadley and York resembles the indirect deuteron spectra obtained in the present experiment.

E. Evidence for the Indirect Pickup Process

The argument given in the next section and in Appendix I about surface nucleons depends on the fact that the deuterons observed in this experiment are formed by the indirect pickup process. Because of this a summary is given here of the evidence supporting this viewpoint.

1. The strongest evidence indicating that the indirect pickup process is the mechanism producing the deuterons observed lies in the A dependence of the deuteron cross section for light elements (see Eqs. 28 and 29).

$$\sigma_{p+x\rightarrow d}(40^{\circ}) = k\, A^{1.2}$$

The exponent 1.2 not only shows that the process must be a two step one but this exponent agrees with the exponent expected for the indirect pickup process. The indirect pickup process is the simplest two step process for making deuterons that is applicable in this case.

2. The deuteron energy spectra and the deuteron angular distribution obtained by the method outlined in Section IV fit all the experimental data satisfactorily. This method is a direct application of the indirect pickup process.

In the light of this evidence it would seem very likely that the indirect pickup process is the mechanism responsible for the formation of the deuterons observed.

F. Surface Nucleons

Using the method outlined in Appendix I, we obtained values for the fraction of "surface" nucleons that are neutrons (= x). Actually the surface as defined by this experiment has depth. It is the region in which the pickup part of the indirect pickup process takes place. A rough estimate of the depth of this "surface" can be made. Bransden arrived at a total deuteron production cross section in carbon of 9mb by assuming a deuteron producing layer of thickness 1.4×10^{-13} cm thick and considering only deuterons having energy larger than 41 Mev. An approximation to the total cross section in carbon measured in this experiment might be $\left[1.8 \frac{\text{mb}}{\text{ster}}\right] (2\pi) = 11.3$ mb. Assuming that this cross section is larger than Bransden's, because the value Bransden chose for the thickness of the deuteron producing layer was too small, we would arrive at a value of 1.75×10^{-13} cm for the thickness of this layer.

The values of x are shown on Fig. 24. The crosses are the volume fraction of nucleons that are neutrons. This is given by

$$\frac{\text{number of neutrons}}{\text{atomic number}} = \frac{N}{A}$$

The experimental values of x for light elements (lithium and carbon) lie on the curve of $\frac{N}{A}$ indicating that for light elements the surface nucleons are no different from the nucleons in the rest of the nucleus. For heavier elements, expecially lead and uranium, the experimental value of x lies significantly above the $\frac{N}{A}$ curve. The average of the x values for the four heaviest elements lies almost three standard deviations above the $\frac{N}{A}$ line. This indicates that there is an excess of neutrons on the nuclear surface.

If we take a simple model and assume that there is a nuclear skin composed of neutrons only, we can get an estimate of the thickness of this skin.

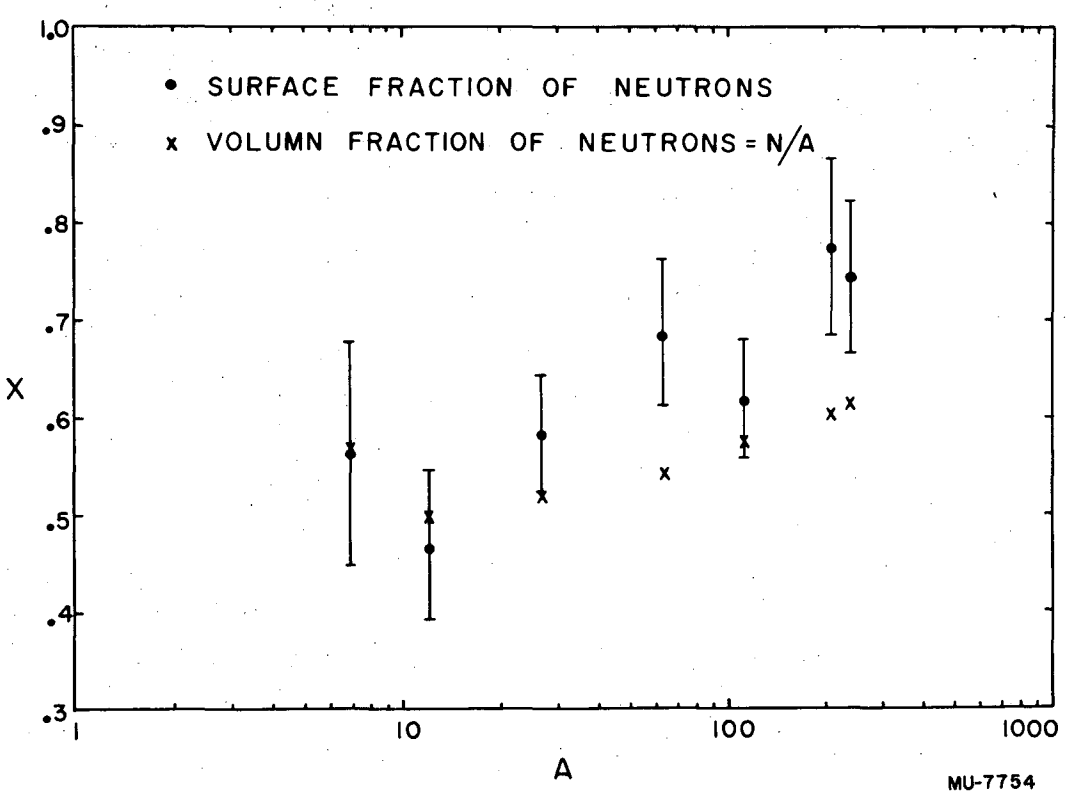

Fig. 24 The Fraction of Surface Nucleons that are Neutrons for Various Elements.

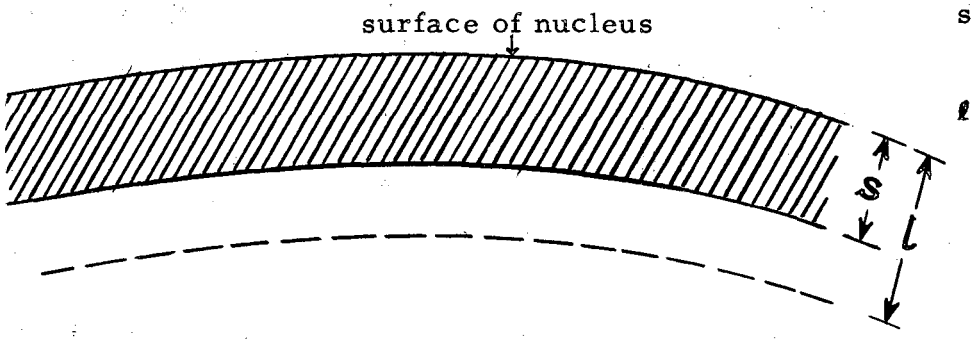

s = neutron skin thickness

ℓ = deuteron producing layer thickness

$$\ell x = s\,1 + (\ell - s)\,\frac{N}{A} \tag{34}$$

For Pb this becomes

$$(1.75 \times 10^{-13})\,(0.78) = S + (1.75 \times 10^{-13} - S)\,0.6 \tag{35}$$

$$S = 0.8 \times 10^{-13}\ \text{cm}$$

This says then that the neutron skin increases from zero thickness for light elements to about 0.8×10^{-13} cm for heavy elements. Undoubteldy this skin actually contains some protons also. In this case, the assumed skin thickness must be increased somewhat to maintain the right value of x.

Measurements of nuclear radii by methods that involve the charge distribution[24] and by methods that involve the nuclear potential distribution[25] tend to substantiate this viewpoint. The charge distribution radius seem to be smaller, thus suggesting the presence of surface neutrons; but it is quite hard to make a direct comparison of different radii determinations. The shape of the nuclear charge distribution for gold has recently been measured quite accurately at Stanford.[26] At present very little is known about the exact shape of the nuclear potential distribution. Lacking this

knowledge we must compare average or root mean square radii. The best value of the square well radius coefficient from the charge distribution experiments[24] is about $r_o = 1.20 \times 10^{-13}$ cm and for the nuclear distribution the value is abour $r_o = 1.37 \times 10^{-13}$ cm. The value of r_o is the coefficient in the expression for the nuclear radius.

$$R = r_o A^{\frac{1}{3}}$$

The charge distribution radius is smaller, but part of the difference should be due to the range of nuclear forces besides the neutron skin effect. Neglecting the effect of the range of nuclear forces, we can get a value for the neutron skin thickness from these data. Considering lead,

$$S = \Delta r_o A^{\frac{1}{3}} = (207)^{\frac{1}{3}} (1.37 - 1.20) \times 10^{-13} = 1.0 \times 10^{-13} \text{ cm} \qquad (36)$$

This is compatible with the value found in the present experiment.

The neutron skin effect has also been postulated theoretically.[7] If one assumes that the nuclear part of the potential well is the same for protons and neutrons (this charge independence idea is quite well accepted, especially at low energies) then the coulomb potential for protons is the only difference in the potentials. The figure below shows this situation.

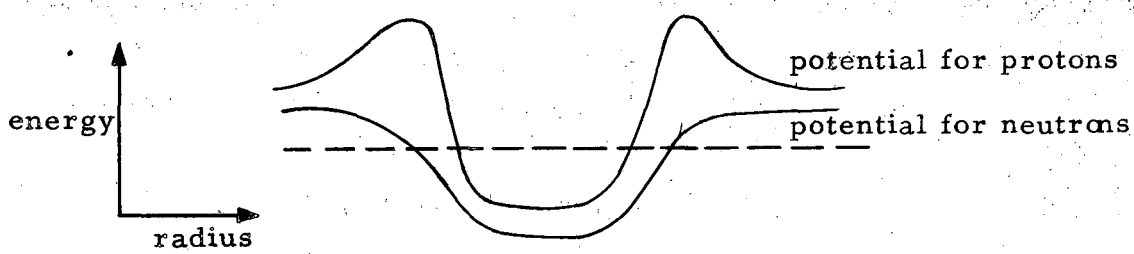

The dotted line shown on the figure is the highest filled level for both neutrons and protons. These levels must lie less than 1 Mev apart, because nuclei are β-stable.

If the nuclear potential has a slope near the surface (as is drawn for the neutron potential) the potential well is effectively narrower for protons than for neutrons. There are theoretical reasons to believe that

the nuclear potential does have a slope near the surface.[27] If the potential well for protons is smaller than for neutrons, then the protons are more limited in space and there is a neutron skin. The thickness of the skin in this case can be estimated by saying that the difference in the radii of the proton and neutron wells for heavy elements is something like $\frac{1}{2}$ of the width of the sloping part of the well. If the sloping part of the well is due to nuclear forces its width is about the Compton wave length of a π meson. This can be seen from the uncertainty principle assuming that the virtual emission of π mesons is responsible for this sloping part of the well.

$$\Delta E \, \Delta t \sim \hbar \tag{32}$$

$$(m_\pi c^2) \, \Delta t \sim \hbar$$

The time Δt is the time during which a virtual meson can be emitted and not violate the uncertainty principle. In this time, assuming it travels with the velocity of light, it moves a distance X.

$$\Delta t = \frac{x}{c} \sim \frac{\hbar}{m_\pi c^2}$$

$$x \sim \frac{\hbar}{m_\pi c} \sim 2 \times 10^{-13} \text{ cm}$$

This would give a neutron skin of about

$$S \sim (\tfrac{1}{2}) \, (2 \times 10^{-13}) = 1 \times 10^{-13} \text{ cm} \tag{38}$$

This argument, while only qualitative, agrees quite well with the other information at hand.

G. Tritons

As shown in the mass spectrum in Fig. 13, there is a measurable yield of tritons observed at wide angles to a 300 Mev nucleon beam. Cross sections for triton production are given in Tables I and II. The A dependence of the triton cross sections measured at 40° to the beam is shown in Fig. 16. If we perform a least squares fit to the data for Li, C, and Al we get

$$\sigma_{p+x\rightarrow t}(40^{\circ}) = 0.0075\ A^{1.22} \tag{39}$$

$$\sigma_{n+x\rightarrow t}(40^{\circ}) = 0.0059\ A^{1.35} \tag{40}$$

This A dependence is very similar to the deuteron A dependence. This would imply that the tritons also are formed by the indirect pickup process. Another piece of evidence leading to this same conclusion is related to the yield of deuterons and tritons. Hadley and York observed one triton for about every 10 deuterons from C. In this experiment for light elements there is about one triton for 12 deuterons observed. The energy spectrum for tritons from proton bombardment of light elements at 40° to the beam is shown in Fig. 25. This is similar to the deuteron spectra, again indicating that the indirect pickup process is responsible for the triton production.

H. Nucleon Momentum Distribution Inferred from Direct Pickup Deuterons

Chew and Goldberger, using the data of Hadley and York, derived a nucleon momentum distribution. Chew and Goldberger felt at the time of the analysis that their momentum distribution might not be very accurate for large values of the momentum. Quoting them

> "The agreement with experiment is satisfactory except for a group of low energy deuterons whose relative number increases with angle. These could easily be of a secondary origin, i.e., the result of interactions between three or more particles. A typical process

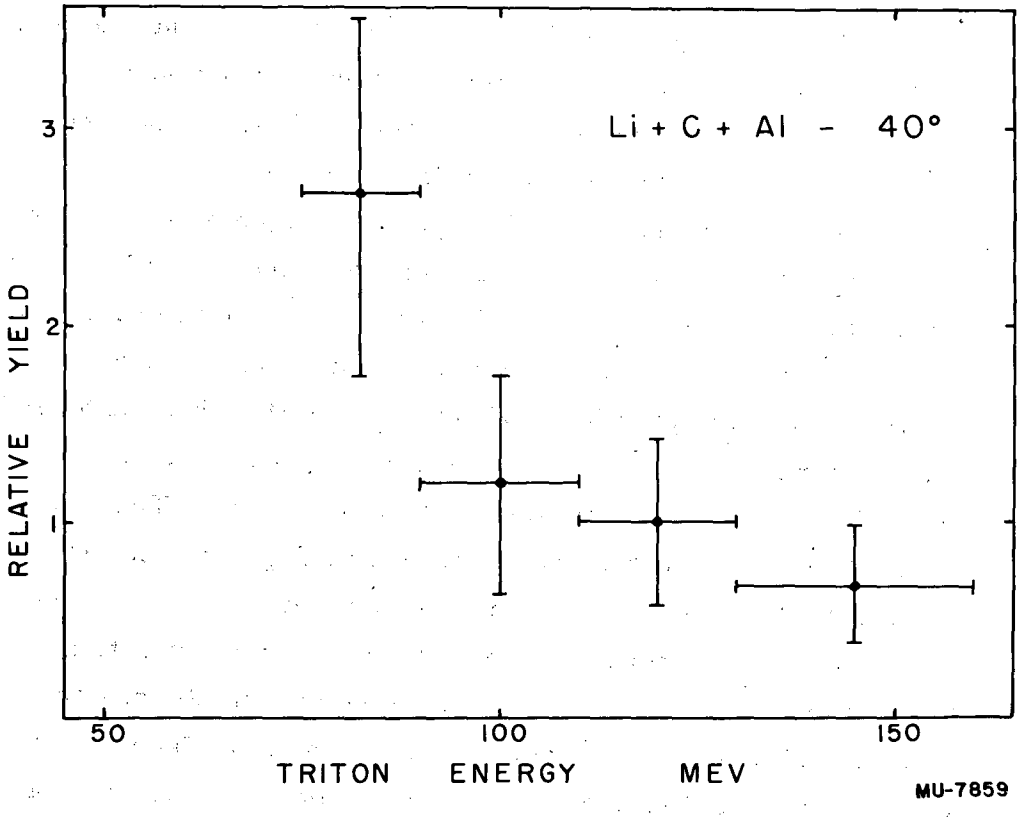

Fig. 25 Energy Spectrum of Tritons at 40° to the Beam for Light Elements Bombarded with 300 Mev Protons.

> of this type, which seems fairly likely, is to have a fast proton, produced in an exchange collision, pick up a neutron from the same nucleus. Since the incident neutron will not have lost all its energy in the initial collision, the emerging deuteron will have a smaller momentum than those considered in this paper. Such secondary deuterons should be smaller in number than the fast protons observed in the same bombardment and be less peaked in angular distribution. The data is inadequate at present to check such facts. Practically all of York's 45° deuterons could be secondary, and we may have seriously overestimated the high momentum components of the proton wave function in attempting to fit at this angle."

It now appears that there is, as suggested, a competing reaction for producing deuterons. The presence of indirect pickup deuterons would confuse the analysis. A reexamination of the data of Hadley and York using the same method as Chew and Goldberger was made. This is a simple kinematics problem, which relates the yield of 62 Mev deuterons at the several angles measured to the number of nucleons having the respective momenta required by the kinematics. The nuclear momentum distribution derived this way is shown in Fig. 26. If, as is suspected, the deuterons observed by Hadley and York at 45° are predominantly indirect pickup deuterons, then the momentum distribution derived by Chew and Goldberger considering all the observed deuterons to be formed by the direct pickup process contained too many high momentum components. That the Chew and Goldberger distribution contains too many high momentum components seems to be borne out on Fig. 26. A better fit to the experimental data would be the 12 Mev Gaussian. The excited Fermi gas momentum distribution having $E_f = 24$ and $T = 8$ Mev* seems to have too

*The completely degenerate Fermi momentum distribution has been shown by various investigations to contain too few high momentum components. The excited Fermi distribution has been used successfully to fit the data of Cladis, Hadley, and Hess, op. cit., by Doctor Warren Heckrotte and also has been used in an analysis of the pickup process by Heidmann (Phys. Rev. 80, 171 (1950)). The temperature of the Fermi gas in this case is not due to excitation energy but can be attributed to particle interactions (Watanabe Z fur Phys. 113, 482 (1939)).

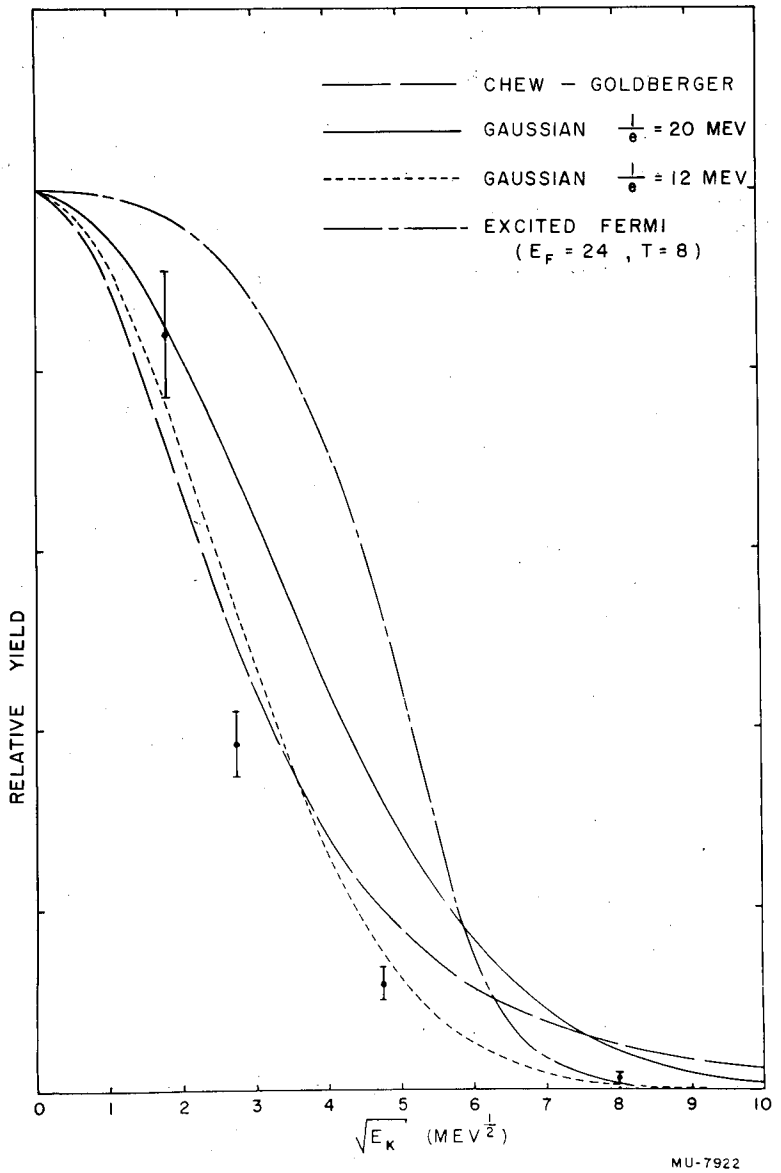

Fig. 26 Nucleon Momentum Distribution Inferred from the Direct Pickup Deuterons observed by Hadley and York.

many intermediate momentum components. If E_f were lowered to about 10 Mev, it would fit better. This might not be unreasonable remembering that the nucleons probed in the direct pickup process are surface nucleons as demonstrated by the A dependence of the cross section. If the nucleus density distribution is not square but has a tail at the edge of the nucleus, then the effective depth of the potential well felt by surface nucleons may be smaller than the average well depth. This would lead to a small Fermi limit.

From this argument, nucleon momentum distributions obtained from an analysis of direct pickup deuterons would contain too few high momentum components because only surface nucleons are involved.

ACKNOWLEDGMENTS

I wish to express my gratitude to Professor Burton Moyer, whose continued guidance and encouragement made the completion of this problem possible.

I would like to thank Dr. Warren Heckrotte for many helpful discussions during the course of the experiment and for making various suggestions concerning the analysis of the data.

Mr. Hoyt Bostick, Mr. Robert Cence and Mr. Fredrick Wikner helped appreciably by reading part of the film.

My thanks also to Dr. Kenneth Bandtel and Mr. Paul Nikonenko for their assistance in building and operating some of the electronics.

Thanks are also due to Mr. James Vale and Mr. Lloyd Houser and the crew of the 184 inch cyclotron for their help in setting up the equipment and operating the cyclotron.

APPENDIX I

From the work of Bransden[4] and also from this experiment, it appears that the cross section for deuteron production from protons bombarding element A can be written as a product of a nucleon scattering cross section and a pickup probability.

$$\sigma_{p+A\rightarrow d}(\theta) = \sigma_{p+A\rightarrow p}(\theta)\,(P_1) + \sigma_{p+A\rightarrow n}(\theta)\,(P_2) \tag{41a}$$

The first term on the right above is the contribution from scattered protons picking up neutrons. The second term is due to scattered neutrons picking up protons. P_1 is the probability for a scattered proton to pick up a neutron to form a deuteron and P_2 is the probability for a scattered neutron to pick up a proton. Similarly, for neutrons bombarding element A we can write the following:

$$\sigma_{n+A\rightarrow d}(\theta) = \sigma_{n+A\rightarrow p}(\theta)P_1 + \sigma_{n+A\rightarrow n}(\theta)\,P_2 \tag{41b}$$

Now if we separate the scattering in nucleus A into scattering from protons and neutrons we can write

$$\sigma_{p+A\rightarrow p}(\theta) = (f)\,(Z)\,\sigma_{p+p\rightarrow p}(\theta) + (f)\,(A - Z)\,\sigma_{p+n\rightarrow p}(\theta), \tag{42a}$$

$$\sigma_{n+A\rightarrow p}(\theta) = (f)\,(Z)\,\sigma_{n+p\rightarrow p}(\theta), \tag{42b}$$

$$\sigma_{p+A\rightarrow n}(\theta) = (f)\,(A - Z)\,\sigma_{p+n\rightarrow n}(\theta), \tag{42c}$$

$$\sigma_{n+A\rightarrow n}(\theta) = (f)\,(A - Z)\,\sigma_{n+n\rightarrow n}(\theta) + (f)\,(Z)\,\sigma_{n+p\rightarrow n}(\theta). \tag{42d}$$

The subscripts on the cross sections on the right in the above equations mean the following:

Incident Particle + Struck Nucleon in Nucleus→Observed Scattered Particle

The cross sections on the right above are nucleon - nucleon cross sections averaged over a range of energies due to the internal momentum of the struck nucleon. The effect of multiple collisions on the scattered particles along their path out of the nucleus has been included in these cross sections.

In these equations f is a number less than 1 which corrects for attenuation of the beam of incident particles going through the nucleus. Because the mean free paths for neutrons and protons in nuclear matter are nearly the same,[17] the same f is used for both neutrons and protons.

In the course of the experiment we measure four cross sections.

$$\sigma_{p+A\to d}(\theta) \quad , \quad \sigma_{p+A\to p}(\theta)$$

$$\sigma_{n+A\to d}(\theta) \quad , \quad \sigma_{n+A\to p}(\theta)$$

Using this data and above equations, we must make two simplifying assumptions in order to proceed.

$$\sigma_{n+n\to n}(\theta) = \sigma_{p+p\to p}(\theta) \tag{43}$$

$$\sigma_{p+n\to p}(\theta) = \sigma_{n+p\to p}(\theta) = \sigma_{p+n\to n}(\theta) = \sigma_{n+p\to n}(\theta) \tag{44}$$

Equation 43 says that n - n forces are the same as p - p forces. There is considerable evidence in favor of this. Equation 44 says that the n - p differential cross section in the center of mass system is symmetrical about 90°. This is believed to be true in the case of free n - p collisions[28] for angles from 40° cm to 140° cm. The fact that these events take place in the nucleus rather than as isolated events should not change the picture appreciably.

The effect of multiple collisions on these cross sections, as mentioned earlier, probably does not affect the validity of the assumptions much. As before, the mean free paths for protons and neutrons are similar and therefore the changes introduced by multiple collisions should

cancel when ratios of these cross sections are used. For simplicity we shall call the cross section in Eq. 43 σ_{pp} and in Eq. 44 σ_{np}. These should not be taken to be free nucleon - nucleon cross sections.

Substituting into Eq. 41, we get

$$\sigma_{p+A\to d}(\theta) = f\,Z\,\sigma_{pp}\,P_1 + f\,(A - Z)\,\sigma_{np}\,P_1 + f\,(A - Z)\,\sigma_{np}\,P_2 \qquad (45a)$$

$$\sigma_{n+A\to d}(\theta) = f\,Z\,\sigma_{np}\,P_1 + f\,(A - Z)\,\sigma_{pp}\,P_2 + f\,Z\,\sigma_{np}\,P_2 \qquad (45b)$$

Now let us consider the pickup probabilities.

$$P = k\,N \qquad N = \text{number of available partner nucleons} \qquad (46)$$

k = proportionality constant (includes matric element)

The proportionality constant, k, is the same for a proton picking up a neutron as for a neutron picking up a proton.

$$P_1 = k\,N_1 \qquad (47a)$$

$$P_2 = k\,N_2 \qquad (47b)$$

$$N_1 = V\rho\,x \qquad (48a)$$

$$N_2 = V\rho\,(1 - x) \qquad (48b)$$

N_1 = number of available neutrons
N_2 = number of available protons
V = effective nuclear volume for pickup
ρ = nuclear density at V
x = fraction of nucleons in V that are neutrons

The volume V is known to be on the nuclear surface from the A dependence of the deuteron cross sections. Therefore, the nucleons involved in X are surface nucleons. Substituting into Eq. 45 and taking a ratio, we get:

$$R = \frac{\sigma_{p+A\rightarrow d}(\theta)}{\sigma_{n+A\rightarrow d}(\theta)} = \frac{\left[Z\,\sigma_{pp} + (A - Z)\,\sigma_{np}\right] x + (A - Z)\,\sigma_{np}\,(1 - x)}{Z\,\sigma_{np}\,x + \left[(A - Z)\,\sigma_{pp} + Z\sigma_{np}\right](1 - x)} \tag{49a}$$

or

$$R = \left(\frac{Z}{A - Z}\right) \frac{x + \left[1 + \left(\frac{A - Z}{Z}\right)\left(\frac{\sigma_{pp}}{\sigma_{np}}\right)\right](1 - x)}{\left[\left(\frac{Z}{A - Z}\right)\left(\frac{\sigma_{pp}}{\sigma_{np}}\right) + 1\right] x + (1 - x)} \tag{49b}$$

Taking the ratio of the measured proton production cross section

$$S = \frac{\sigma_{p+A\rightarrow p}(\theta)}{\sigma_{n+A\rightarrow p}(\theta)} = \frac{Z\,\sigma_{pp} + (A - Z)\,\sigma_{np}}{Z\,\sigma_{np}} = \frac{\sigma_{pp}}{\sigma_{np}} + \frac{A - Z}{Z} \tag{50}$$

substituting Eq. 50 into Eq. 49 and solving for X, we get:

$$X = \frac{\left(\frac{Z}{A - Z}\right) + S - \left(\frac{A - Z}{Z}\right) - R}{\left[R\left(\frac{Z}{A - Z}\right) + 1\right]\left(S - \frac{A - Z}{Z}\right)} \tag{51}$$

This shows that we can find the fraction of "surface" nucleons that are neutrons from the cross sections measured in this experiment.

REFERENCES

1. D. D. Clark, private communication.
2. J. Hadley and H. York, Phys. Rev. 80, 345 (1950).
3. G. F. Chew and M. L. Goldberger, Phys. Rev. 77, 470 (1950).
4. B. H. Bransden, Proc. Phys. Soc. A 65, 738 (1952); and private communication.
5. Cladis, Hess, and Moyer, Phys. Rev. 87, 425 (1952).
6. P. A. Wolff, "The Inelastic Scattering of Protons from Carbon", Thesis, University of California Radiation Laboratory, Report No. UCRL-1410, July, 1951; and Phys. Rev. 87, 434 (1952).
7. M. H. Johnson and E. Teller, Phys. Rev. 93, 357 (1954).
8. C. E. Leith, Phys. Rev. 78, 89 (1950).
9. Bruno Rossi, High Energy Particles (Prentice Hall, New York, 1952) pp. 29-35.
10. Taylor, Jentschke, Remley, Eby, and Kruger, Phys. Rev. 84, 1034 (1951).
11. Chamberlain, Segrè, and Wiegand, Phys. Rev. 83, 923 (1951). J. DePangher, "A High Pressure Cloud Chamber Investigation of Proton Scattering by 300 Mev Neutrons", Thesis, University of California Radiation Laboratory, Report No. UCRL-2153, March, 1953.
12. W. Selove, Phys. Rev. 92, 1328 (1953); and private communication.
13. J. Heidmann, Phys. Rev. 80, 171 (1950).
14. A. Bratenahl, private communication.
15. L. M. Slater, "High Energy (d,p) Reactions", Thesis, University of California Radiation Laboratory, Report No. UCRL-2441, March, 1954.
16. Fernbach, Serber, and Taylor, Phys. Rev. 75, 1352 (1949).
17. A. J. Kirschbaum, "Nuclear Absorption Cross Sections for High Energy Protons", Thesis, University of California Radiation Laboratory, Report No. UCRL-1967, October, 1952; and Phys. Rev. 90, 449 (1953).
18. W. J. Knox, Phys. Rev. 81, 687 (1951). J. A. Hoffman and K. Strauch, Phys. Rev. 90, 449 (1953). F. Mandl and T. H. R. Skyrme, AERE Harwell TR 745.

19. G. N. Temmer, Phys. Rev. 83, 1057 (1951).

20. D. D. Clark, "Elastic Scattering of 340 Mev Protons by Deuterons", Thesis, University of California Radiation Laboratory, Report No. UCRL-2255, June, 1953.

21. R. Serber, Phys. Rev. 72, 1008 (1947).

22. S. M. Dancoff, Phys. Rev. 72, 1017 (1947).

23. R. N. Stuart, "The Effect of the External Coulomb Field on Deuterons Produced in Nuclei", University of California Radiation Laboratory, Report No. UCRL-2574.

24. Lyman, Hanson, and Scott, Phys. Rev. 84, 626 (1951). V. L. Fitch and J. Rainwater, Phys. Rev. 92, 789 (1953). F. Bitter and H. Feshbach, Phys. Rev. 92, 837 (1953).

25. Cook, McMillan, Peterson, and Sewell, Phys. Rev. 75, 7 (1949). Bratenahl, Fernbach, Hildebrand, Leith, and Moyer, Phys. Rev. 77, 597 (1950). Warren Heckrotte, "Nuclear Cross Sections and the Size of the Nucleus", University of California Radiation Laboratory, Report No. UCRL-2510, March, 1954.

26. Hofstadter, Fechter, and McIntryre, Phys. Rev. 91, 422 (1953); and to be published.

27. J. M. C. Scott, Phil. Mag. 45, 441 (1954).

28. Chung Ying Chih, "A Cloud Chamber Study of the Scattering Cross Section of Protons by 90 Mev Neutrons at Extreme Angles", Thesis, University of California Radiation Laboratory, Report No. UCRL-2575, May, 1954. J. DePangher, op. cit.